Optical Second Harmonic Generation as a Probe of Surface Chemistry

Robert M. Corn* and Daniel A. Higgins

Department of Chemistry, University of Wisconsin—Madison, 1101 University Avenue, Madison, Wisconsin 53706

Received April 6, 1993 (Revised Manuscript Received July 19, 1993)

Contents

I. Introduction

Optical second harmonic generation (SHG) is the nonlinear conversion of two photons of frequency ω to a single photon of frequency 2ω which, in the electric dipole approximation, requires a noncentrosymmetric medium. The ability of noncentrosymmetric crystals to produce SHG has led to their implementation as frequency doublers in a wide variety of laser systems. SHG can also be obtained from the break in symmetry that occurs at the interface between two centrosymmetric media. Since only the first few atomic or molecular monolayers on either side of the interface participate in this symmetry breaking, the SHG process can be used as a highly surface-selective optical probe of interfacial phenomena.[1]

Shortly after the initial SHG measurements of Franken et al. in 1961,[2] the sensitivity of SHG to the interface between two centrosymmetric media was experimentally demonstrated by Brown, Parks, and Sleeper.[3] In a series of papers, Bloembergen and coworkers determined the theoretical equations that govern SHG from surfaces in a reflection geometry,[4,5] from a thin slab of nonlinearly active material,[4] and finally from the interface of two centrosymmetric media.[6] In the last case, it was assumed that the discontinuity in the electric fields at the interface led to a quadrupolar term in the nonlinear polarization that resulted in SHG from the interface. However, in 1969 Brown and Matsuoka demonstrated that the SHG from a silver surface was highly sensitive to the presence of adsorbed layers.[7] In this work, Brown and Matsuoka proposed that the observed sensitivity was due to an additional surface dipole term in the nonlinear polarization. Rudnik and Stern subsequently presented a new theoretical description of SHG from interfaces between centrosymmetric media in which the surface sensitivity of SHG was primarily attributed to the symmetry-breaking nature of the surface rather than the quadrupolar effects of the previous theories.[8] From these initial works, SHG has evolved into a powerful surface technique that has been widely applied. The extensive application of SHG to the study of surfaces is a direct result of its tremendous sensitivity and selectivity to the interfacial region.

This review presents an extensive overview of the current literature on the application of SHG to the study of surface chemistry. A number of fine reviews on the different aspects of SHG at surfaces have appeared in the past few years.[9-21] We have chosen to concentrate on the most recent works in the field (primarily after 1988) and to present some examples of chemical processes at interfaces that have been studied with the surface SHG technique. Our presentation will include a discussion of some general theoretical concepts that are used to interpret the results of the SHG experiments, along with a brief summary of the experimental requirements for surface SHG measurements. The various examples of surface SHG studies have been divided according to the type of chemical information obtained from the particular experiment.

II. Sources of SHG at Interfaces

The generation of second harmonic light at frequency 2ω from an interface can be described using a model of the sample as a collection of N electrons, each in a slightly anharmonic potential field, under the influence of an external fundamental light field of frequency ω.[1,22] For metals, this model can be used to approximate the response from the nearly free electrons at the surface (an extension of Drude theory). For a monolayer of molecules adsorbed to a surface, this model can be viewed as a very simple picture of the valence electrons that lead to the molecular nonlinear optical response. A description of the motion $x(t)$ for one of the electrons is given in the following equation:

$$\ddot{x} + \omega_0^2 x + \zeta x^2 = \frac{e}{m}\{E(\omega)\cos(\omega t)\} \qquad (1)$$

where ω_0 and ζ are the resonant frequency and anharmonicity of the potential field, $E(\omega)$ is the magnitude of the oscillating electric field associated with the incident fundamental light, and all other symbols have their usual meaning. The motions of the collection of electrons under the influence of this oscillating electric field give rise to a macroscopic time-dependent polarization $P(t) = \sum_N ex(t)$. The Fourier component of this polarization at frequency 2ω, $P^{(2)}(2\omega)$, is responsible for the SHG from the sample and is proportional to the square of the amplitude of the incident electric field:

$$P^{(2)}(2\omega) = \chi^{(2)}E^2(\omega) \qquad (2)$$

The proportionality constant $\chi^{(2)}$ is called the second-order nonlinear susceptibility, and is given in this simple

0009-2665/94/0794-0107$14.00/0

Robert M. Corn was born in Honolulu, HI, in 1956. He received a B.A. in Chemistry summa cum laude in 1978 from the University of California, San Diego. In 1983, he received his Ph.D. in Chemistry from the University of California, Berkeley, under the direction of Professor Herbert L. Strauss. His thesis work was on the application of Fourier-transform infrared spectroscopy to the study of molecular solids. After completing his degree, he spent a year and a half as a Visiting Scientist at the IBM Research Laboratory in San Jose, CA, where he applied the techniques of Raman scattering and optical second harmonic generation to electrochemical surfaces. Following IBM, he spent a year as a Visiting Assistant Professor in the area of Physical Chemistry at Swarthmore College in Swarthmore, PA. In 1985, he moved to the University of Wisconsin—Madison, where he is currently an Associate Professor in the Department of Chemistry. His research interests include the application of optical second harmonic generation, polarization–modulation Fourier-transform infrared spectroscopy, Raman scattering, and surface plasmons to the study of electrochemical interfaces, self-assembled monolayers, and organic thin films.

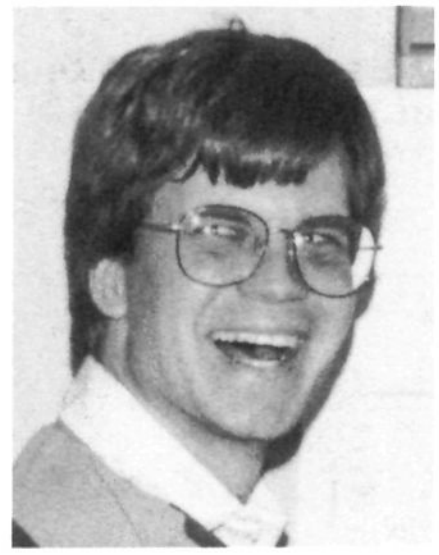

Daniel A. Higgins was born in Columbia, MO, in 1966 and grew up in Brookings, SD, and later in Eden Prairie, MN. He graduated magna cum laude from St. Olaf College in Northfield, MN, with a B.A. in Chemistry in 1988 and has been attending graduate school at the University of Wisconsin—Madison in the Department of Chemistry since that time. His doctoral research is being performed under the direction of Professor Robert M. Corn and involves the study of molecular adsorption and orientation on surfaces with optical second harmonic generation. He was awarded the Charles N. Reilley—Upjohn Award for Outstanding Research in Analytical Chemistry in 1990. Following his expected graduation from the Ph.D. program this fall, he will be working with Professor Paul Barbara at the University of Minnesota in the area of femtosecond spectroscopy.

description by the following equation:

$$\chi^{(2)} = -\zeta \frac{Ne^3}{2m^2} \frac{1}{(\omega_0^2 - \omega^2)^2 (\omega_0^2 - 4\omega^2)} \quad (3)$$

Note that $\chi^{(2)}$ has several important properties:

(i) $\chi^{(2)}$ is proportional to the anharmonicity constant ζ. This is the realization of the symmetry requirements for SHG in the electric dipole approximation. If ζ is zero, the potential becomes symmetric and there is no SHG. For metals, theoretical calculations have shown that the magnitude of $\chi^{(2)}$ from the interface depends critically on the shape of the electron density profile at the surface.[23–38] For molecular systems, only those molecules which have an asymmetric electron density distribution (either inherent or induced by adsorption to a surface) will be capable of yielding a surface second harmonic response.

(ii) $\chi^{(2)}$ has resonances at frequencies ω_0 and $(^1/_2)\omega_0$. The second harmonic response from a metal surface when both the fundamental and second harmonic frequencies are below the plasma frequency (ω_0) is sometimes referred to as "nonresonant SHG" in reference to the weak wavelength dependence expected for the SHG from the surface.[19] At frequencies above ω_0, resonance effects should be observed in the surface second harmonic response. In addition, real metals possess complex band structures that contain optical interband transitions and surface-state excitations which can also potentially lead to resonant enhancement effects and wavelength dependencies in the surface second harmonic response.[37,39–45]

When in resonance with an electronic transition in an adsorbed molecule, the SHG from the interface is often dominated by adsorbate contributions to $\chi^{(2)}$. This molecular surface second harmonic response is sometimes referred to as "resonant SHG".[46] The magnitude and polarization dependence of the resonant SHG response from a monolayer of adsorbed molecules depends upon the average molecular orientation at the surface and the intrinsic nonlinear optical response of the molecules. This response is described by the molecular nonlinear polarizability tensor β and can be calculated theoretically.[1,47–49]

(iii) In this model, $\chi^{(2)}$ is proportional to N, the number of electrons in the system. For molecules, this means that $\chi^{(2)}$ of an adsorbed monolayer will depend linearly on the surface concentration. Similarly for metals, the $\chi^{(2)}$ of the surface will be directly related to the surface concentration of free electrons. An extension of this relation is that the SHG should vary inversely with the work function of the metal surface. A number of authors have exploited this relation in a semiquantitative fashion.[39,50–54] In general, it is observed that adsorbates which donate electrons to the metal surface (e.g., hydrogen, alkali metals) increase the surface second harmonic response, whereas adsorbates which accept electrons from the metal surface (e.g., oxygen) generally decrease the amount of SHG from the surface.

When the preceding derivation of the surface nonlinear susceptibility $\chi^{(2)}$ is generalized for application to three-dimensional systems, $\chi^{(2)}$ becomes a third-rank tensor. The second harmonic intensity $I(2\omega)$ from any interface in either reflection or transmission geometry is proportional to the square of $\chi^{(2)}$:

$$I(2\omega) = \frac{32\pi^3\omega^2 \sec^2\theta_{2\omega}}{c^3} |\mathbf{e}(2\omega)\cdot\chi^{(2)}\cdot\mathbf{e}(\omega)\mathbf{e}(\omega)|^2 I^2(\omega) \quad (4)$$

where $\theta_{2\omega}$ is the angle from the surface normal at which the SHG signal occurs, the vectors $\mathbf{e}(\omega)$ and $\mathbf{e}(2\omega)$ describe the fundamental and second harmonic light

fields at the surface, and all other symbols have their usual meaning. This equation has been derived by Heinz[18] and by Mizrahi and Sipe.[55]

As implied in eq 4, the surface nonlinear susceptibility $\chi^{(2)}$ is a third-rank tensor which in general can have 18 distinct nonzero complex elements, χ_{IJK}, where I, J, and K refer to Cartesian axes defined with the surface normal as the $+Z$ direction. For most systems, the number of nonzero elements is greatly reduced by the surface symmetry. For example, if the surface is rotationally isotropic about the surface normal, as in the case of a nonchiral liquid surface, there are only three distinct independent nonzero tensor elements: χ_{ZZZ}, $\chi_{ZXX} = \chi_{ZYY}$, and $\chi_{XXZ} = \chi_{XZX} = \chi_{YYZ} = \chi_{YZY}$. For single-crystal metal or semiconductor surfaces, additional tensor elements are allowed and SHG experiments can be used to probe the average surface symmetry as described below.

The description of the surface nonlinear susceptibility discussed above is valid only in the electric dipole approximation. It should be noted that the SHG signal from an interface arises from the sum of surface electric dipole, bulk magnetic dipole, bulk electric quadrupole, and higher order contributions. Although the additional terms cannot be neglected a priori, it is often assumed or determined experimentally that they do not contribute significantly to the surface second harmonic response. However, in certain cases the contributions of the higher order surface and bulk terms to the overall nonlinear polarizability are important; these cases have been discussed in the literature.[56-58]

III. General Experimental Considerations

Since the second harmonic response of an interface is proportional to the square of the incident light intensity, surface SHG measurements normally employ high-powered pulsed-laser systems. A schematic of the typical experimental apparatus used in surface SHG studies is shown in Figure 1. A nanosecond or picosecond pulsed laser is usually the source of the fundamental light. The output of the laser is polarized, filtered to remove any extraneous second harmonic light, and sometimes focused onto the sample. Typical power densities on the surface range from 10^5 to 10^8 W cm^{-2}, depending on the nonlinear susceptibility and damage threshold of the surface. The SHG created at the surface is analyzed with a second polarizer and separated from the fundamental light by filters and a small monochromator. The second harmonic photons are detected with a photomultiplier tube and the overall second harmonic intensity is measured with either a boxcar averager or gated photon counting electronics.[59,60] Conversion efficiencies are normally very small, on the order of 10^{-12}%. Thus, the observed SHG signal from surfaces typically ranges from 5 to 50 000 photons s^{-1}, depending on the laser and surface employed. A small piece of the fundamental beam is often diverted to a reference channel that creates an SHG signal from a second source. The output of the reference channel is used to normalize the surface SHG signal and remove the effects of any fluctuations in the laser power during the course of the experiment.

Surface SHG experiments can be performed in either a reflection or transmission geometry. (The latter, of course, will only work for transparent substrates.)

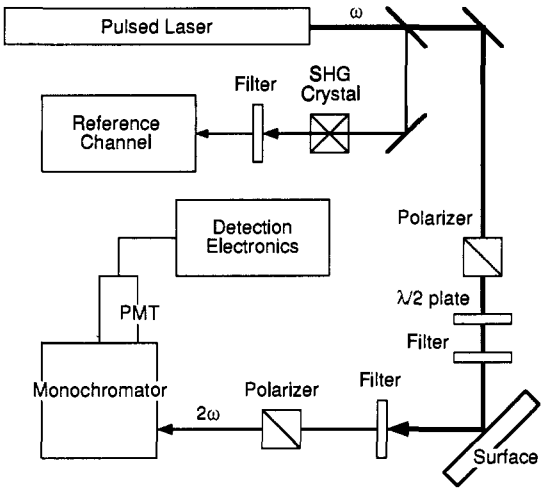

Figure 1. The SHG experimental apparatus. A high-powered pulsed laser is usually employed as the light source. A small portion of the laser beam is sent to a reference channel which is used to remove laser fluctuations, while the majority of the beam is sent to the sample surface to create the surface SHG signal. The fundamental laser light is usually linearly polarized and filtered prior to impinging on the sample. Typical angles of incidence range between 30° and 70° from the surface normal. The sample can consist of a solid–gas, solid–liquid, liquid–gas, or liquid–liquid interface. The second harmonic beam is easily separated from the fundamental laser light by filters and a monochromator. The detection electronics typically consist of either gated photon counting electronics or a boxcar averager.

Typical angles of incidence for the fundamental beam range from 30° to 70° with respect to the surface normal. For an isotropic surface, no SHG is observed at an incident angle of 0° (normal incidence). The second harmonic created at the interface is phase matched to the incident fundamental light in the plane of the surface. Therefore, for surfaces in air or in UHV, the SHG beam is coincident with the reflected fundamental beam; however, for more dispersive media the two beams need not be collinear. A more complicated phase-matching arrangement arises if the SHG experiment is performed with two fundamental beams.[61] Additional experimental details specific to a particular surface SHG measurement are elaborated separately in the following sections.

IV. SHG Measurements of Surface Chemistry

The sensitivity and selectivity of the SHG technique has led to its application in the study of surface chemistry for a large number of interfacial systems. The surface nonlinear susceptibility, $\chi^{(2)}$, is directly related to the structure of the interface and can be determined from measurements of the magnitude, polarization dependence, and phase of the SHG from the surface. What is measured in most surface SHG experiments is a change in $\chi^{(2)}$ upon adsorption to some new value $\chi'^{(2)}$. This change can be formally separated into two parts:[19,56]

$$\chi'^{(2)} = \chi^{(2)} + \chi_A^{(2)} + \Delta\chi_I^{(2)} \quad (5)$$

where $\chi_A^{(2)}$ is the inherent nonlinear susceptibility of the adsorbate and $\Delta\chi_I^{(2)}$ is the change in nonlinear susceptibility of the surface due to any interactions with the adsorbate. SHG experiments utilizing either

$\chi_A^{(2)}$ or $\Delta\chi_I^{(2)}$ have been applied to metal, semiconductor, oxide, polymer, and liquid surfaces. These experiments can be categorized by the type of information obtained from the surface SHG studies: (i) adsorption strength and surface coverage, (ii) molecular orientation, (iii) surface symmetry, (iv) interfacial electric field strength, and (v) reaction kinetics and surface diffusion.

A. Adsorption and Surface Coverage Measurements

Most surface SHG experiments monitor the adsorption of a species to an interface via changes in the surface second harmonic response. While these changes can always be used in a qualitative manner to observe an adsorption process, in some cases the SHG measurements can be used as a quantitative measure of adsorption strength and surface coverage. In these instances the modifications to the surface nonlinear susceptibility are related to changes in the relative surface coverage, θ, where θ is equal to Γ/Γ_T, the adsorbate surface coverage divided by the maximum surface coverage observed for the species. For systems where the nonlinear optical response of an adsorbate dominates the surface SHG, θ is monitored via $\chi_A^{(2)}$. At other interfaces the relative surface coverage of an adsorbed species is probed indirectly via changes in the surface nonlinear susceptibility ($\Delta\chi_I^{(2)}$). The various classes of interfaces at which the adsorption and reaction of surface species have been monitored with SHG experiments are examined separately in further detail below.

1. Metal Surfaces in UHV

The original SHG measurements of adsorption to metal surfaces in vacuum were performed by Brown and Matsuoka in 1969,[7] who reported that the amount of SHG from a silver surface changed dramatically upon adsorption of contaminants. Over a decade later, Tom et al. published the first application of SHG measurements to single-crystal metal surfaces in UHV; in these studies, the authors used SHG to investigate the adsorption of O, CO, and Na onto Rh(111) surfaces.[62,63] Since these initial efforts, the application of SHG to studies of adsorption at metal surfaces in UHV has expanded considerably and to date includes studies of adsorption onto Ag,[64-68] Cu,[44,69-71] Pt,[39] Pd,[42,72] Ni,[39,73-78] Al,[29,79,80] Re,[53,54,81] and Rh.[82]

The SHG from the surface of metals is almost always dominated by the nonlinear polarizability of the free and bound metal electrons at the interface. Any changes in the amount of surface SHG upon adsorption of a molecule or atom onto the metal surface are usually related to changes in the nonlinear optical response of the surface electronic states. A number of researchers have attempted detailed theoretical descriptions of the changes in the SHG response of the surface upon chemisorption,[28,32,38,83] but have only produced qualitative results. Most experimental studies still rely on empirical models similar to the anharmonic oscillator theory described in section II. As mentioned in that secton, in some instances the SHG signal can be related to the free-electron surface density and the work function of the metal surface.[39,51-54]

Whatever the mechanism, the changes observed in the SHG from a metal surface upon adsorption can be formally described as a change in the surface nonlinear susceptibility, $\Delta\chi_I^{(2)}$. If the changes are sufficiently small, then $\Delta\chi_I^{(2)}$ will depend linearly on the relative surface coverage θ of the adsorbed species. An example of this relationship can be seen in Figure 2, in which the SHG signal from a Ni(110) surface is plotted as a function of CO surface coverage.[78] The solid line in Figure 2 is a fit of the experimental data using the assumption of a linear decrease in $\chi^{(2)}$ with increasing θ_{CO}. Further theoretical and experimental work is needed in this area to relate the SHG measurements in a detailed fashion to the electronic structure of the metal surface.

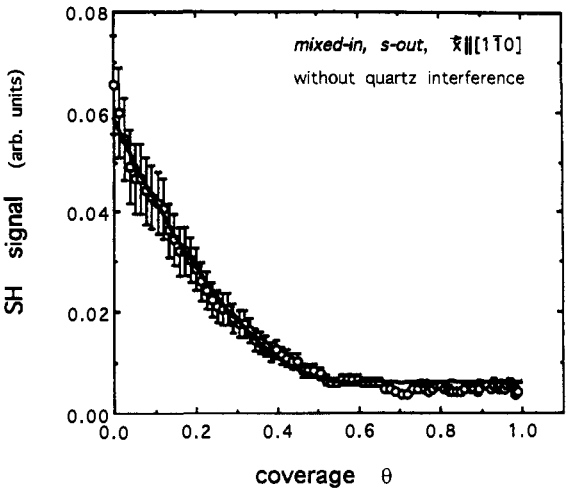

Figure 2. The SHG signal from a Ni(110) surface in UHV as a function of θ, the relative surface coverage of CO. The solid line is a fit of the experimental SHG data assuming that $\Delta\chi_I^{(2)}$ varies linearly with θ (see eq 5). (Reprinted from ref 78. Copyright 1991 American Physical Society.)

2. Metal-Electrolyte Interfaces

At solid-liquid interfaces, the unique symmetry requirements of the SHG process result in a surface *selectivity* (as well as sensitivity) that is not attainable with any linear spectroscopic method. For this reason, SHG is an ideal spectroscopic technique for examining electrochemical interfaces and has been employed to study the adsorption of molecules, ions, metal atoms, and reaction intermediates at metal electrodes.[9-21] SHG has also been used to characterize the surface enhancement of electromagnetic fields at roughened noble metal electrodes;[14] these experiments are not covered in this review. SHG measurements of surface symmetry, surface reconstruction, and electrostatic fields at metal electrodes are discussed separately in sections C and D.

As in the UHV studies, the SHG from the metal-electrolyte interface is dominated by the nonlinear optical response of the metal surface. Changes in the metal surface nonlinear susceptibility ($\Delta\chi_I^{(2)}$) due to adsorption are used to indirectly monitor the relative surface coverage of chemisorbed species. In the absence of any specific electronic resonances, the chemisorption of species which increase the surface density of free electrons results in an increase in the surface SHG. In contrast, adsorbates which decrease the surface free-electron density lead to a reduction of the SHG from the interface. This indirect method of monitoring chemisorption limits the chemical selectivity of these

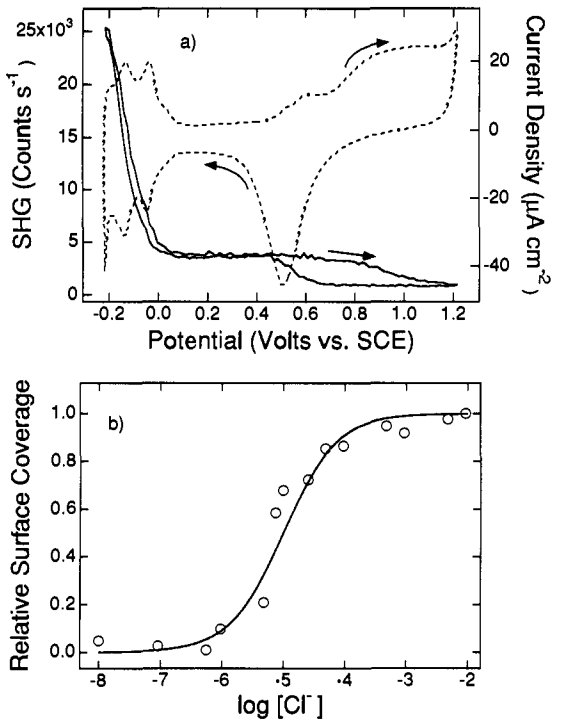

Figure 3. (a) The SHG (solid line) and cyclic voltammogram (dashed line) from a polycrystalline platinum electrode immersed in a 0.5 M $HClO_4$ and 1 mM KCl solution as a function of applied potential (vs SCE). The dramatic increase in the SHG at potentials below 0.0 V is due to the absorption of monatomic hydrogen. In the double-layer region between 0.0 and 0.4 V, the SHG remains at a nonzero, potential-independent value that is attributed to the adsorption of chloride ions. Above 0.4 V, the chloride is removed from the surface and is replaced by an oxide layer, resulting in a lower SHG signal level. Panel b shows the adsorption isotherm for chloride ions at a potential of 0.2 V, as determined from the surface SHG signal from the polycrystalline platinum electrode described in Figure 3a. The solid line is a fit of the data to a Frumkin isotherm. (Reprinted from ref 116. Copyright 1990 American Chemical Society.)

measurements. However, the in situ information obtained from these experiments is extremely difficult to acquire by any other method. For this reason, SHG experiments have been used frequently to study chemisorption onto Ag,[10,11,84-100] Cu,[70,101,102] Au,[103-114] Pt,[59,115-119] Fe,[120,121] Ni,[122,123] and Hg[124] electrodes.

An example of the application of SHG to the study of adsorption on metal electrode surfaces is shown in Figure 3a, in which the SHG obtained during the electrochemical cycling of a polycrystalline platinum electrode in a 0.5 M $HClO_4$ and 1 mM KCl solution is plotted.[116] Hydrogen atoms, chloride ions, and an OH or oxide monolayer are chemisorbed onto the platinum surface at various potentials during the electrochemical cycle. The chemisorption of each of these species can be monitored with the changes in the surface second harmonic response.

At potentials below 0.0 V vs saturated calomel electrode (SCE), a large increase in the SHG is observed due to the adsorption of a monatomic hydrogen species. SHG experiments have provided information on hydrogen adsorption at Ag,[91] Cu,[102] and Pt[115,117-119] electrodes. In particular, the controversial adsorption of hydrogen onto Pt(111) single-crystal electrodes[125] has been verified with SHG measurements.[117]

At potentials above 0.4 V vs SCE, Figure 3a shows a decrease in the SHG from the platinum surface due to the formation of an oxide or OH monolayer. This decrease in surface SHG is consistent with the results of UHV experiments of oxygen adsorption onto Pt(111) surfaces.[39] The formation of oxides has also been found to affect the SHG signal from Ag,[86,88] Au,[126] Cu,[70] Fe,[121] and Ni[122] electrodes.

At potentials between 0.0 V and 0.4 V, chloride ions are chemisorbed onto the platinum electrode. The amount of SHG observed in Figure 3a at these potentials depends upon the amount of chloride chemisorbed onto the surface. Figure 3b plots the relative surface coverage of chloride (θ_{Cl}) at 0.2 V determined from the SHG experiments as a function of chloride concentration in solution. The surface coverage of chloride was obtained by assuming a linear relationship between $\Delta\chi_I^{(2)}$ and θ_{Cl}, and that $\theta_{Cl} = 1$ at the highest solution concentration. Bromide and iodide adsorption onto Pt electrodes has also been monitored with SHG measurements.[116,119] In addition, anionic adsorption has been studied extensively at Ag,[89,90,95] Cu,[101,102] and Au[108,112,113] electrodes.

3. Semiconductor Surfaces

SHG experiments employing GaAs and Si crystals in a reflection geometry represent some of the earliest examples of surface SHG measurements.[5] The analysis of the second harmonic response in these early experiments aided in the development of the macroscopic theoretical description of nonlinear optical effects at interfaces. The first systematic application of SHG to the study of adsorption at semiconductor surfaces was performed by Chen et al., who monitored the adsorption of alkali metals onto Ge in UHV.[50,127] Since those initial experiments, the vast majority of SHG measurements of adsorption onto semiconductor surfaces has been performed on Si surfaces. Specific works have included studies on the chemisorption of H,[128] P,[129] Ba,[130] Ge,[131,132] Ga,[133-136] As,[136,137] and Au[138-140] onto Si surfaces in UHV. Several authors have also studied the formation and removal of oxide layers on Si.[141,142] In addition, Heinz et al. have used SHG measurements to probe the CaF_2–Si interface.[143] SHG measurements have also been used to study adsorption onto Ge[144] and noncentrosymmetric GaAs surfaces.[145-151] In the majority of these measurements, adsorption was monitored through the contributions of $\Delta\chi_I^{(2)}$ to the surface nonlinear susceptibility.

4. Oxide and Insulator Surfaces

In contrast to metal and semiconductor surfaces, it is often the case for insulating oxide surfaces (e.g., fused silica) that the inherent nonlinear susceptibility of the surface is small. In these systems, the molecular SHG from an adsorbate, $\chi_A^{(2)}$, can dominate the surface susceptibility; this is particularly true if the adsorbed molecules are specifically designed with a large nonlinear polarizability and if the SHG is resonantly enhanced by the selection of fundamental or second harmonic wavelengths near a molecular electronic transition. The SHG from these surfaces will be proportional to the square of the surface concentration of the adsorbed molecules, as long as the average molecular orientation and the molecular nonlinear polarizability of the adsorbate does not change as a function of surface coverage.

The use of resonant SHG as a quantitative measure of molecular adsorption on oxide surfaces was first demonstrated by Heinz et al. for the adsorption of *p*-nitrobenzoic acid at the fused silica–ethanol interface.[152] Subsequent studies of adsorption have been performed for a variety of molecules at fused silica surfaces in air,[49,152-161] ethanol,[162,163] and chloroform.[49] In addition to silica surfaces, SHG has also been employed to monitor adsorption onto a variety of other insulator surfaces.[164-167]

In some cases the surface nonlinear susceptibility depends on the surface coverage of an adsorbed molecule in a more complicated fashion. For example, it has been shown for large dye molecules that molecular aggregation within the monolayer leads to large local field effects[168,169] which result in a nonlinear dependence of $\chi_A^{(2)}$ on the surface coverage.[156,161,170] In addition, for molecules with small nonlinear polarizabilities, or in cases where the molecular response is not resonantly enhanced, the small amount of SHG from the substrate surface cannot always be neglected.[157,171-173]

In some instances the second harmonic response of the surface is dominated by $\chi^{(2)}$ of the substrate. As in the case of metal or semiconductor surfaces, molecular adsorption must then be monitored through $\Delta\chi_I^{(2)}$. This type of measurement has been utilized to study the adsorption of water onto alkali halide crystals[174,175] and the adsorption of polymers onto mica surfaces.[176,177]

A topic related to the adsorption of molecular monolayers onto oxide surfaces is the preparation of noncentrosymmetric thin films for nonlinear optics. Two excellent books discussing the design of molecules for such systems have recently been published.[178,179] Films of these molecules are typically prepared on nonconducting substrates, such as fused silica, by a Langmuir–Blodgett dipping process or by spreading from a volatile solvent followed by a rubbing procedure. These films can range in thickness from submonolayer up to microns. Since the preparation of nonlinear optical materials is reviewed elsewhere,[178,179] we will not discuss the properties of these films in any detail. However, interfacial SHG measurements of adsorption and surface coverage have been used to monitor the formation of a wide variety of monolayers of these materials, as well as the extent of molecular orientation and order within the monolayers.[166,180-206]

5. Liquid–Air Interfaces

One interface for which a wealth of new information has been obtained with surface SHG measurements is the liquid–air interface. The first observation of SHG from a liquid–air interface was by Wang in 1969,[207] and the first quantitative measurements of surface coverage and molecular orientation on monolayers at the water–air interface were performed by Rasing et al. on Langmuir films.[208,209] Since these initial experiments, SHG has been used extensively to examine the adsorption equilibrium between solute molecules at the interface and in the bulk liquid. As in the case of oxide surfaces, the contributions of the organic adsorbates to the surface nonlinear susceptibility ($\chi_A^{(2)}$) usually dominate the surface second harmonic response. A typical example of an SHG measurement of surface coverage at a liquid–air interface is shown in Figure 4.

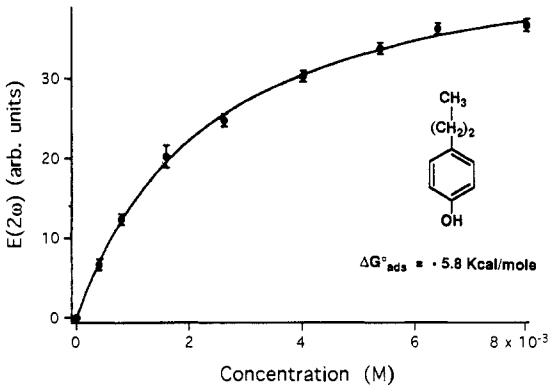

Figure 4. The square root of the second harmonic intensity, $E(2\omega)$, from a water–air interface as a function of *p*-propylphenol concentration in the aqueous phase. The solid line is the best fit to a Langmuir isotherm for adsorption of *p*-propylphenol to the interface. Results of this type can be used to determine the energetics of adsorption; in this case, the free energy of adsorption is determined to be -5.8 kcal/mol. (Reprinted from ref 210. Copyright 1991 American Institute of Physics.)

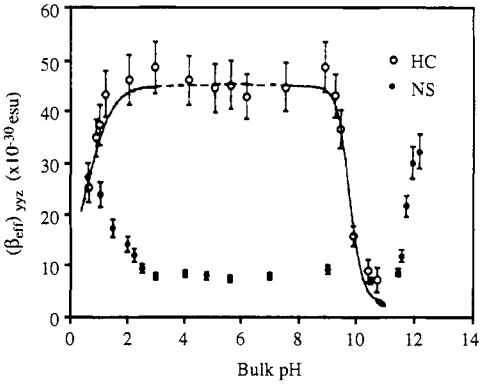

Figure 5. The experimentally determined effective molecular nonlinear polarizability, $(\beta_{eff})_{yyz}$, for hemicyanine (HC) and nitrostilbene (NS) dye molecules at the water–air interface as a function of pH. The solid line is a theoretical fit to the data. Both dye molecules are coadsorbed with stearic acid. The pH-dependent variations in $(\beta_{eff})_{yyz}$ are attributed to the protonation and deprotonation of the various acid–base groups of each molecule. Acid–base reactions effect the charge transfer resonances in the dye molecules and lead to dramatic changes in the amount of SHG from the surface. (Reprinted from ref 170. Copyright 1991 American Institute of Physics.)

In this work by Castro et al.,[210] the authors examined the adsorption of a series of alkylphenol and alkylaniline molecules to the water–air interface. The dependence of $\chi_A^{(2)}$ on the bulk concentration of an adsorbate was used to determine the adsorption isotherm, and thus the free energy of adsorption to the interface. Similar experiments have been performed for other molecules at liquid–air interfaces.[49,211-221]

The molecular specificity provided by $\chi_A^{(2)}$ has led to the application of SHG in the study of chemical transformations at interfaces. Changes in the molecular nonlinear polarizability upon the reaction of an adsorbed molecule will result in changes in the surface second harmonic response. Xiao et al.[170] have observed changes in the SHG from hemicyanine and nitrostilbene monolayers at the water–air interface as a function of the pH in the bulk aqueous phase; the results of this work are plotted in Figure 5. The changes in the SHG from the interface as a function of pH are attributed to the protonation/deprotonation of the acid–base sites

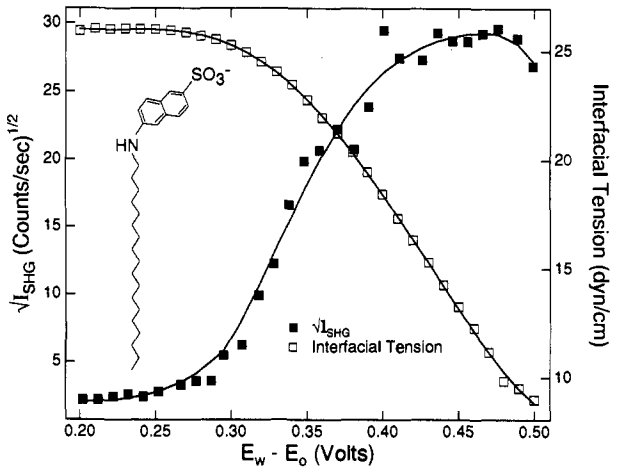

Figure 6. The square root of the second harmonic intensity, $\sqrt{I_{SHG}}$ (filled squares), and the interfacial tension (open squares) from an electrified water–1,2-dichloroethane interface as a function of the applied potential E_w–E_o. The solid lines are drawn to show the trends in the data. The dichloroethane contains 20 μM of an anionic surfactant 2-(*N*-octadecylamino)naphthalene-6-sulfonate (ONS) which adsorbs to the liquid–liquid interface. The increase in the SHG is due to the potential-dependent adsorption of ONS to the interface and is accompanied by a decrease in the interfacial tension. These results were used quantitatively to obtain thermodynamic information on the adsorption of ONS. (Reprinted from ref 60. Copyright 1993 American Chemical Society.)

on the molecules. Reactions of this type result in changes in the electronic structure of the molecule and shifts in the strength and position (energy) of the charge-transfer bands. These shifts lead to dramatic variations in the amount of SHG observed from the interface. The populations of protonated and deprotonated species are easily monitored with the surface SHG signal, thus allowing for the elucidation of pH differences between the surface region and the bulk solution. Several other pH-dependent studies of this type have appeared recently.[155,222-224] Studies involving the use of time-resolved SHG measurements to probe the kinetics of surface reactions have also been reported and will be discussed in section E.

6. Liquid–Liquid Interfaces

Molecular adsorption to liquid–liquid interfaces can also be monitored with the SHG from the interface. The first detailed SHG study of a liquid–liquid interface was performed by Grubb and co-workers for the adsorption of an anionic surfactant at the decane–water and water–carbon tetrachloride interfaces.[225] Subsequent studies have been performed at water–heptane interfaces,[226] silver metal liquidlike films at water–organic interfaces,[227] and most recently, liquid–liquid electrochemical interfaces.[60] An example of the information that can be obtained from the liquid–liquid electrochemical interface is shown in Figure 6, which plots the potential dependent SHG from an anionic surfactant at the water–1,2-dichloroethane interface.[60] At potentials where the dichloroethane side of the interface is negatively charged, the anionic surfactant is strongly adsorbed to the interface, and a large SHG signal is observed. Conversely, when the dichloroethane side of the interface is positively charged, the surfactant is driven away from the interface, resulting in a complete loss of the surface SHG signal. An analysis of the SHG results, in conjunction with surface tension measurements, can provide a very accurate description of the interfacial energetics. In addition to adsorption measurements, surface reactions can be followed through the changes in the surface SHG signal. This has been demonstrated for a photoinduced electron transfer reaction at a liquid–liquid interface.[228]

B. Molecular Orientation Measurements

In addition to the numerous applications of interfacial SHG to the study of molecular adsorption, SHG experiments have been frequently utilized to determine the average orientation of molecules adsorbed at surfaces. For systems where the SHG from the interface is dominated by molecular contributions to the surface nonlinear susceptibility ($\chi_A^{(2)}$), the average orientation of the molecules at the interface can be obtained from measurements of the polarization dependence and phase of the molecular SHG. The current methodology for these molecular orientation measurements is an extension of the original experiments by Heinz et al. in the early 1980s.[46,152]

The SHG molecular orientation measurement incorporates three main steps: first, the magnitudes and relative phases of the surface nonlinear susceptibility tensor elements are measured; second, the nonlinear response of an individual molecule is calculated or assumed; and third, the average molecular orientation at the interface is calculated through the appropriate equations relating the experimentally measured macroscopic surface nonlinear response to the expected microscopic molecular nonlinear response. In some cases, an additional step involving the measurement of the phase of the surface second harmonic response with respect to the fundamental light fields can be used to ascertain the absolute molecular direction of the molecules adsorbed onto the surface.

1. Molecular Orientation Determination Methodology

The average molecular orientation within an adsorbed monolayer is determined from the polarization dependence of the surface SHG signal $I(2\omega)$. This polarization dependence is stated formally in eq 4 and depends upon the relative magnitudes and phases of the elements of the surface nonlinear susceptibility tensor $\chi^{(2)}$ as well as the input and output polarization vectors $\mathbf{e}(\omega)$ and $\mathbf{e}(2\omega)$. Explicit equations for the polarization vectors for a variety of experimental geometries can be found in papers by Heinz,[18] Sipe,[55] and Marlow[163] and are based on the Fresnel factors for the interface.

If the SHG from the adsorbed monolayer is invariant during rotation of the surface about the surface normal (the Z axis), then the molecules within the laser spot are randomly oriented about the surface normal and $\chi^{(2)}$ has only three unique elements: χ_{XXZ}, χ_{ZXX}, and χ_{ZZZ}. The intensity of the s-polarized (perpendicular to the plane of incidence) and p-polarized (parallel to the plane of incidence) SHG signal ($I_s(2\omega)$ and $I_p(2\omega)$, respectively) can be directly related to these elements:

$$I_s(2\omega) \propto |a_1\chi_{XXZ} \sin^2\gamma|^2 I(\omega)^2 \qquad (6)$$

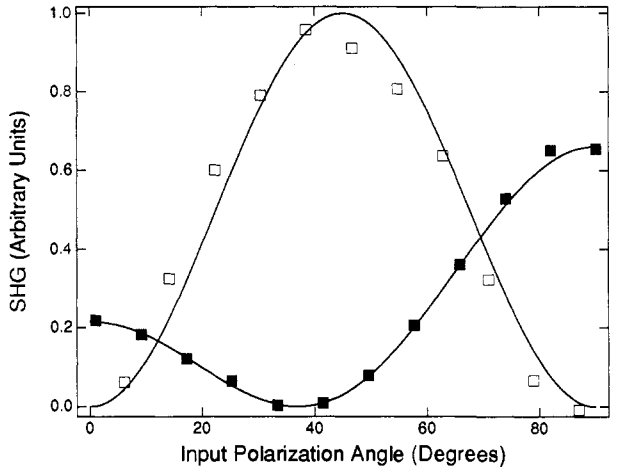

Figure 7. The polarization dependence of the s-polarized SHG, $I_s(2\omega)$ (open squares), and the p-polarized SHG, $I_p(2\omega)$ (filled squares), from a monolayer of *p*-nitrophenol adsorbed at the silica–air interface. The input polarization of the fundamental beam is defined as 0° for p-polarized light and 90° for s-polarized light. The solid lines are fits to eqs 6 and 7 and are used to obtain values for χ_{XXZ}, χ_{ZXX}, and χ_{ZZZ} from the surface. These tensor elements are used to determine the molecular orientation within the monolayer. (Reprinted from ref 49. Copyright 1992 American Chemical Society.)

$$I_p(2\omega) \propto |(a_2\chi_{XXZ} + a_3\chi_{ZXX} + a_4\chi_{ZZZ}) \cos^2\gamma + a_5\chi_{ZXX} \sin^2\gamma|^2 I(\omega)^2 \quad (7)$$

where γ is the polarization angle of the incident light ($\gamma = 0°$ for p-polarized light and $\gamma = 90°$ for s-polarized light). The a_i terms include combinations of the components of $\mathbf{e}(\omega)$ and $\mathbf{e}(2\omega)$ and the dielectric constants of the monolayer, $\epsilon'(\omega)$ and $\epsilon'(2\omega)$.[49,55,229] Guyot-Sionnest et al. have stressed the need for an independent measurement of $\epsilon'(\omega)$ and $\epsilon'(2\omega)$ in order to obtain an accurate picture of the molecular orientation.[230] In addition, local field corrections must be included in a rigorous interpretation of the SHG polarization dependence.[168,169] An example of polarization dependent SHG measurements is shown in Figure 7, in which $I_p(2\omega)$ and $I_s(2\omega)$ are plotted as a function of γ for a monolayer of *p*-nitrophenol adsorbed at a fused silica–air interface.[49] From this data, the relative magnitudes of the various $\chi^{(2)}$ elements for the monolayer were obtained via eqs 6 and 7. Estimates of the monolayer dielectric constants used in these equations were obtained through a Kramers–Kronig analysis of the UV–vis absorption experiments.[49,160]

In order to obtain average molecular orientation information from the polarization dependence of the surface SHG, knowledge of the complex second-order molecular nonlinear polarizability tensor β for an isolated molecule is required. This tensor describes the nonlinear polarization at frequency 2ω ($\alpha^{(2)}(2\omega)$) that is induced in a molecule by an incident laser light field $\mathbf{E}(\omega)$:

$$\alpha^{(2)}(2\omega) = \beta:\mathbf{E}(\omega)\mathbf{E}(\omega) \quad (8)$$

Using perturbation theory, the components of β can be expressed in terms of the molecular energies and wave functions.[47] In many of the molecular orientation studies to date, this rather complicated equation has been approximated by assuming that the molecular nonlinear response is governed only by the lowest energy

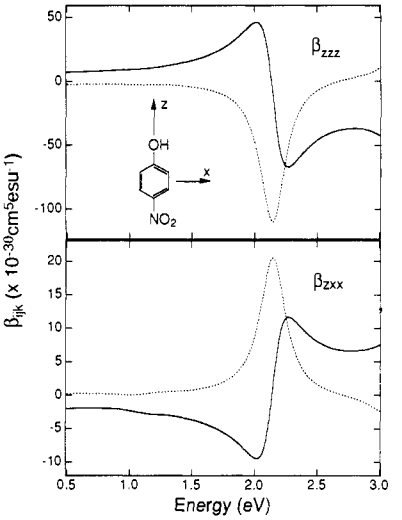

Figure 8. Semiempirical π-electron calculation for the molecular nonlinear polarizability tensor elements β_{zzz} and β_{zxx} of *p*-nitrophenol as a function of fundamental photon energy. β_{zzz} and β_{zxx} are defined with respect to the molecular axes depicted in the figure and were found to be the dominant tensor elements at energies corresponding to the UV–vis spectral region. Both the real (—) and imaginary (- - -) tensor components are shown. (Reprinted from ref 49. Copyright 1992 American Chemical Society.)

electronic resonance in the molecule and, therefore, can be considered as a two-level system:[231]

$$\beta_{ijk} = \frac{-e^3}{2\hbar^2}\left[\frac{\Delta r_n^i r_{ng}^j r_{ng}^k}{\omega_{ng}^2 - \omega^2} + r_{ng}^i(r_{ng}^j \Delta r_n^k + \Delta r_n^j r_{ng}^k)\frac{\omega_{ng}^2 + 2\omega^2}{(\omega_{ng}^2 - 4\omega^2)(\omega_{ng}^2 - \omega^2)}\right] \quad (9)$$

where β_{ijk} is the tensor element referenced to the molecular coordinate axes i, j, and k; ω is the incident laser frequency; $\hbar\omega_{ng}$ is the energy difference between excited state n and the ground state g; Δr_n^i is the difference in the permanent dipole moment between the excited state and the ground state; and r_{ng}^i is the transition dipole matrix element between the two states along the molecular i axis. The molecular nonlinear polarizability β has several important properties: (i) as in the anharmonic oscillator presented in section II, β has resonances at ω_{ng} and $(1/2)\omega_{ng}$; (ii) the nonzero elements of β will always lie in a plane prescribed by the transition dipole moment and the change in dipole moment upon excitation; and (iii) if the transition dipole moment and the change in dipole moment are collinear, β_{zzz} will be the only nonzero molecular nonlinear polarizability tensor element.

For the majority of molecules chosen for SHG studies to date, it has been assumed that only one tensor element β_{ijk} dominates the molecular nonlinear response. This assumption has been made for small molecules like *p*-nitrobenzoic acid (β_{zzz} dominant)[152] as well as for larger dye molecules such as rhodamine 6G (β_{zxx} dominant).[46] However, it has been shown that the two-level approximation is not always valid, and that in many instances a second tensor element of β must be included in the orientation calculation.[49,59,160,226,232] For example, Figure 8 plots β_{zzz} and β_{zxx} as a function of fundamental photon energy for *p*-nitrophenol. These results were calculated from the

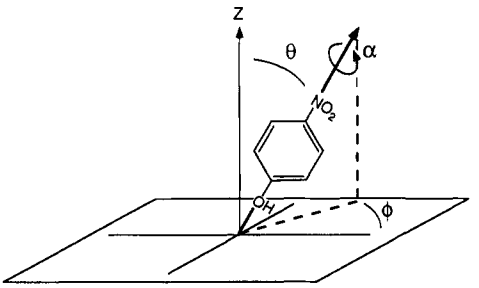

Figure 9. Definition of the angles α, ϕ, and θ employed in the molecular orientation calculation. The surface normal is defined as the laboratory Z axis. The molecular orientation distribution in ϕ is usually assumed to be random; this assumption can be verified experimentally by demonstrating that the surface SHG is isotropic with respect to rotation of the surface about the Z axis.

semiempirical π-electron wave functions obtained from a Pople–Pariser–Parr SCF-CI methodology.[48,233-237] Although the calculations show that at visible wavelengths β_{zzz} is the largest β tensor element, there is also a nonnegligible contribution from β_{zxx}. It has been shown that both of these tensor elements must be included in the molecular orientation calculation for p-nitrophenol in resonant SHG experiments and that their relative magnitudes can be obtained from the experimentally measured $\chi^{(2)}$ elements (see below).[49,226]

Once it has been determined which elements of the molecular nonlinear polarizability dominate the molecular nonlinear response, these elements can be related to the experimentally determined tensor elements of $\chi^{(2)}$ through a coordinate transformation from the molecular coordinate system to that of the surface. This mathematical relationship allows for the calculation of the average molecular orientation on the surface and is given by[232]

$$\chi_{IJk} = N_s \sum \langle R_{Ii} R_{Jj} R_{Kk} \rangle \beta_{ijk} = N_s \sum \langle F_{IJkijk}(\phi,\theta,\alpha) \rangle \beta_{ijk} \quad (10)$$

where N_s is the surface concentration of adsorbed molecules, and $\langle R_{Ii} R_{Jj} R_{Kk} \rangle$ is the ensemble average of the product of three direction cosines, R_{Xx}, between the laboratory and molecular coordinate systems. The product of direction cosines can be expressed as a function $F_{IJKijk}(\phi,\theta,\alpha)$, where the molecular angles ϕ, θ, and α are defined relative to the space fixed coordinates as shown in Figure 9. For most molecular monolayers, the SHG from the surface does not depend upon the azimuthal angle ϕ. In this case the molecules are oriented randomly about the surface normal and F_{IJKijk} can be integrated over ϕ, leaving a function of θ and α. Further simplification of the function F_{IJKijk} is possible and depends upon which β_{ijk} tensor elements dominate the molecular nonlinear response.

For example, in the molecular orientation calculation for a monolayer of p-nitrophenol adsorbed at the fused silica–air interface,[49] eq 10 can be used to relate the measured values of the elements of $\chi^{(2)}$ to the molecular β elements. The ratio of the two dominant elements β_{zxx}/β_{zzz} derived from this equation is given in eq 11:

$$\frac{\beta_{zxx}}{\beta_{zzz}} = 2\frac{\chi_{ZXX} - \chi_{XXZ}}{\chi_{ZZZ} + 2\chi_{XXZ}} \quad (11)$$

The values of the tensor elements determined from the data in Figure 7 lead to a β_{zxx}/β_{zzz} of −0.31. If it is further assumed that there is a random distribution in the angle α for the adsorbed p-nitrophenol molecules, then a molecular orientation parameter D can be derived from eq 10:

$$D = \frac{\langle \cos^3 \theta \rangle}{\langle \cos \theta \rangle} = \frac{\chi_{ZZZ} - \chi_{ZXX} + \chi_{XXZ}}{\chi_{ZZZ} + 3\chi_{XXZ} - \chi_{ZXX}} \quad (12)$$

Using the values of the tensor elements determined from Figure 7, a value of 0.33 is obtained for D. This D corresponds to an average angle θ of 55° if all of the molecules are sitting on the surface with the same orientation. A concurrent study by Bell et al. on p-nitrophenol at water–air and water–heptane interfaces arrived at a similar result.[226] A more involved interpretation of D that assumes a Gaussian distribution of molecular angles θ has also been discussed.[49,238] The equations for the orientation parameter D in cases where other β tensor elements are dominant have been presented in other review articles.[239]

2. Examples of Molecular Orientation Measurements

As noted above, the original SHG orientation measurements were performed on a rhodamine dye adsorbed at the fused silica–air interface.[46] By assuming a single dominant molecular nonlinear polarizability element, an orientation parameter of $D = 0.69$, corresponding to an average angle θ of 34°, was calculated from the polarization dependence of the surface SHG. Several similar studies on large dye molecules have appeared in the literature.[162,240] Orientation measurements which assume the presence of two molecular nonlinear polarizability tensor elements have been performed on monolayers of the dye molecule methylene blue at fused silica–air[160] and metal–electrolyte[59] interfaces. An interesting extension of the SHG orientation methodology has been reported by Peterson and Harris,[241] in which UV–vis spectroscopy was coupled with SHG orientation studies of rhodamine B monolayers at a fused silica–air interface in order to elucidate the average orientation of dimers adsorbed onto the surface.

Orientation studies of large dye molecules are complicated by the close proximity of several molecular electronic resonances to the fundamental and second harmonic wavelengths. The contributions of multiple electronic transitions in β make the molecular nonlinear polarizability tensor analysis more difficult, but lead to large resonance enhancement of the surface SHG response. The difficulties associated with the larger molecules are avoided in orientation studies of small aromatic molecules like p-nitrophenol. As shown in the β calculation in Figure 8, these molecules can be studied with lasers that provide for resonance enhancement at the second harmonic only. Although the surface SHG signal may be smaller, the orientation analysis of the SHG is often simplified by the presence of only one dominant molecular nonlinar polarizability tensor element, β_{zzz}. Molecules of this nature include p-nitrobenzoic acid,[152] p-nitroaniline, and many others. Many orientation measurements utilizing these small molecules have been performed at fused silica–air,[49,238] water–air,[176,208,209,211,212,216,225,226,229,242-244] and a variety of other interfaces.[225,226]

3. SHG Phase Measurements of Absolute Molecular Orientation

In addition to the measurement of the orientation parameter D from the polarization dependence of the surface SHG, measurements of the phase of the surface second harmonic response can be used to deduce the absolute direction of the adsorbed molecules on the surface. As first demonstrated by Kemnitz et al.,[245] these experiments entail the measurement of the phase of a surface susceptibility tensor element (usually χ_{XXZ}) with respect to the phase of the incident fundamental light fields via an interference method. The phase measurements involve the insertion of a second source of SHG, usually a thin piece of z-cut quartz, into the beam reflected from the sample surface. The residual fundamental light in the beam will generate SHG in the z-cut quartz that is shifted in phase from the SHG generated at the sample surface. By translating the z-cut quartz along the beam path, an interference pattern is produced which includes the desired information on the phase relationship between the surface nonlinear susceptibility and the fundamental light fields. In order to ascertain the phase shift of this interference pattern with respect to the input fields, the system must first be calibrated by replacing the sample with a second piece of z-cut quartz of known orientation and repeating the above interference measurements.[245] Comparison of the observed phase with that predicted from the molecular nonlinear polarizability calculations results in the determination of the absolute molecular direction for the molecules adsorbed to the interface. The original absolute orientation determination was made with phase measurements of the SHG from phenol molecules adsorbed to the water–air interface[245] and has since been applied to adsorbates at other interfaces.[49,246]

As a representative example of this type of measurement, Figure 10a plots the χ_{XXZ} interference curves for the SGH from a p-nitrophenol monolayer adsorbed at the air–water interface (open squares) and a quartz reference (filled squares).[49] The quartz reference in these experiments is known to generate SHG with a phase of –90° with respect to the incident light fields. Therefore, the interference measurements for p-nitrophenol show that at this fundamental wavelength (610 nm), the tensor element χ_{XXZ} is +70° out of phase with respect to the incident light fields. Figure 10b plots the theoretically expected phase of the nonlinear susceptibility element χ_{XXZ} for a monolayer of p-nitrophenol adsorbed with the orientation shown in the figure (the OH group down). These results were calculated from the elements of β that are expected to contribute to the molecular SHG in this wavelength region. As seen in the figure, the phase of χ_{XXZ} is calculated to be 180° below resonance, 90° on resonance, and 0° above resonance. In contrast, if the molecule were oriented with its nitro group down, the phase of χ_{XXZ} would range between 0° and 180° with a value of –90° on resonance. A phase of +70° (from Figure 10a) for χ_{XXZ} indicates that the p-nitrophenol molecules are oriented with the OH group pointing down, into the water.

A different interferometric method for determining absolute molecular orientation has been developed by Sato et al. and involves the interference of the SHG from two monolayers adsorbed on opposite faces of a fused silica substrate.[247,248] The advantage of this method is that the reference sample is another adsorbed layer of the same (or related) molecule; therefore, the phase characteristics of the two monolayers can be matched very closely and lead to a simple interpretation of the data. The sample geometry and experimental setup used in this type of SHG measurement are shwon in Figure 11. By collecting the SHG in transmission through the sample as a function of the angle of incidence, an interference pattern is produced which contains the desired phase relationship between the SHG from the monolayers on either side of the substrate. An example of such an experiment is shown in Figure 12, in which the interference patterns for the two types of hemicyanine monolayer systems shown in Figure 11a are compared to illustrate the utility of the method.

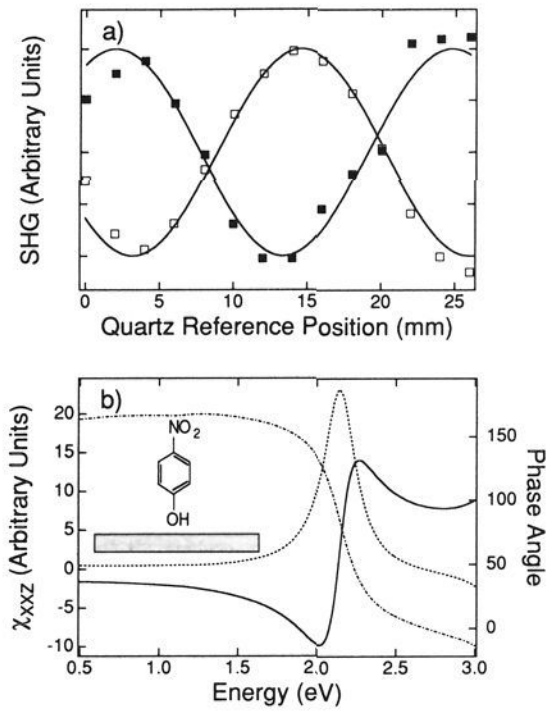

Figure 10. (a) The resonant SHG phase measurement for a monolayer of p-nitrophenol at the air–water interface used to determine the absolute molecular orientation. The open squares are the interference pattern produced by combining the SHG from the adsorbed monolayer with the SHG from a thin slab of z-cut quartz placed in the beam reflected from the surface. The interference pattern is recorded as a function of the position of the z-cut quartz along the beam path. The filled squares are the interference pattern obtained when the sample is replaced by a second piece of z-cut quartz of known orientation. Since the z-cut quartz reference is known to produce SHG with a –90° phase shift with respect to the incident light fields, it is determined from these measurements that the SHG from the p-nitrophenol monolayer has a +70° phase shift. Part b shows the calculation of the magnitudes [both real (—) and imaginary (- - -)], and the phase angle (- · - ·) of the complex surface nonlinear susceptibility element χ_{XXZ} for a monolayer of p-nitrophenol adsorbed at the water–air interface with the OH groups pointing down (into the water) as a function of fundamental photon energy. These theoretical results show that the SHG from a p-nitrophenol monolayer, when exactly on resonance, will have a +90° phase shift in this orientation and imply that the phase measurement of +70° shown in part a of this figure demonstrates that the molecules are adsorbed with their OH groups pointing down. (Reprinted from ref 49. Copyright 1992 American Chemical Society.)

C. Surface Symmetry Measurements

A third major application of surface SHG measurements has been the determination of suface symmetry

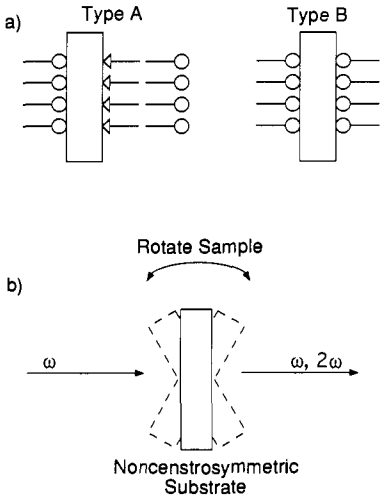

Figure 11. The general experimental methodology used by Sato et al.[248] for SHG interference measurements to determine the absolute orientation of molecules deposited on opposite sides of a centrosymmetric substrate. Part a shows the schematic diagram of the two samples used to generate the SHG interference patterns. The type A sample has two monolayers of nonlinearly active hemicyanine molecules (denoted as) aligned in the same direction (the monolayer is nonlinearly inactive), and the type B sample has the nonlinearly active molecules aligned in opposite directions. Part b shows the experimental geometry used to measure the SHG interference patterns from the two samples described in part a. The SHG at 2ω is collected in transmission through the sample as a function of the angle of tilt off normal incidence.

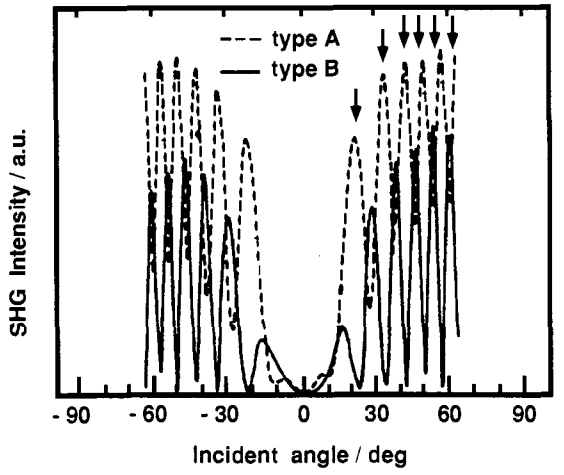

Figure 12. The SHG interference patterns for hemicyanine dye monolayer samples of type A(- - -) and type B (—) as described in Figure 11a as a function of the incident angle on the surface. The two interference patterns are observed to be 180° out of phase due to the inversion of the hemicyanine dye orientation on the surface in type A with respect to type B systems. The arrows indicate the theoretical maxima for films of type A. (Reprinted from ref 248. Copyright 1991 Elsevier Sequoia.)

at single-crystal metal and semiconductor surfaces. As noted above, the number of the 18 possible unique tensor elements χ_{IJK} that can be observed in a particular SHG experiment will depend upon the average symmetry of the surface. Table 1 lists some simple surfaces for a face-centered cubic single crystal, the inherent symmetry of each surface, and the unique nonzero $\chi^{(2)}$ elements expected. More complete listings of the allowed tensor elements for different crystal faces and surface symmetries have been tabulated elsewhere.[14,17,18,56]

Table 1. The Nonzero Elements of $\chi^{(2)}$ Expected for Crystal Faces of Given Symmetry[14,17,18,56]

crystal face	symmetry	nonzero $\chi^{(2)}$ elements
100	C_{4v}	χ_{zzz}, χ_{zxx}, χ_{xxz}
111	C_{3v}	χ_{zzz}, χ_{zxx}, χ_{xxz}, χ_{xxx}
110	C_{2v}	χ_{zzz}, χ_{zxx}, χ_{xxz}, χ_{zyy}, χ_{yyz}

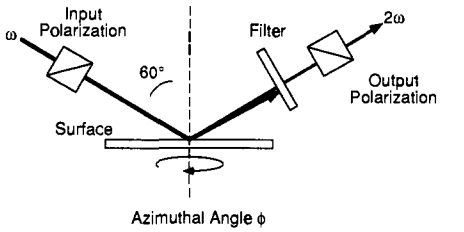

Figure 13. The experimental geometry employed in SHG rotational anisotropy experiments on single-crystal surfaces. The fundamental laser beam is incident on the sample at an angle between 30° and 70°, and the SHG is collected in reflection as a function of crystal rotation about the surface azimuthal angle ϕ. The rotational anisotropy patterns obtained with different input and output polarizations are used to probe the various nonlinear susceptibility tensor elements of a particular single-crystal surface.

The relative magnitudes and phases of the various $\chi^{(2)}$ tensor elements expected for a given single-crystal surface can be determined via SHG rotational anisotropy measurements as depicted in Figure 13. In these experiments, the SHG from the surface is measured at fixed input and output polarizations (usually p- or s-polarization) as a function of azimuthal angle ϕ, where ϕ is determined relative to a particular crystal axis on the surface. Rotational anisotropy measurements at single-crystal surfaces were first demonstrated on Si(111) by Guidotti et al.[249,250] and by Shen and coworkers[251-253] in 1983. Subsequent measurements by Tom and Aumiller demonstrated the utility of the technique at metal single-crystal surfaces, specifically Cu(111).[254] Since these initial measurements, rotational anisotropy measurements have been applied to single-crystal surfaces in air,[255] UHV,[42,70,73-76,137,141,256,257] and electrochemical environments.[41,43,70,100,101,104,108,109,111,113,117-119,256,258-265]

SHG rotational anisotropy measurements are particularly useful for the study of single-crystal metal surfaces in electrochemical environments, as there are exceedingly few techniques that can monitor surface symmetry in situ. The processes of surface disordering, overlayer chemisorption, and surface reconstruction can all potentially lead to changes in the average surface symmetry of an electrode. These symmetry modifications will create new $\chi^{(2)}$ tensor elements, and result in changes in the observed SHG rotational anisotropy. G. Richmond and co-workers at the University of Oregon have pioneered the application of this technique to the study of single-crystal metal electrode surfaces.[10-12,17] Figure 14 depicts SHG rotational anisotropy measurements by Koos and Richmond[111] from a Au(111) electrode with an adsorbed monolayer of Cu, Ag, Tl, or Pb atoms. The process of spontaneous metal monolayer adsorption is denoted by electrochemists as underpotential deposition (upd) and can be used to modify the catalytic properties of an electrode surface.

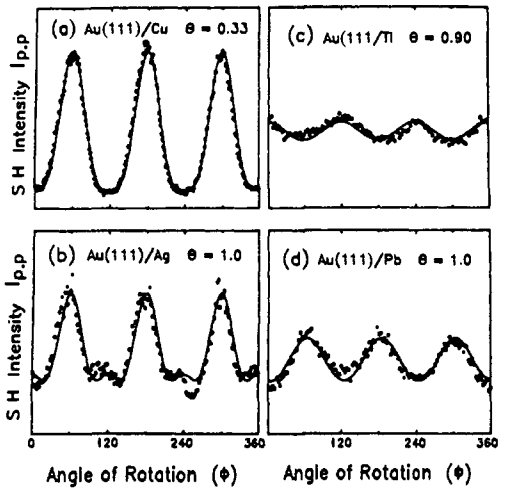

Figure 14. SHG rotational anisotropy measurements of a Au(111) electrode onto which a variety of metal monolayers have been adsorbed by the process of underpotential deposition (upd). The solid lines are fits to theoretical equations. Changes in the surface electronic structure upon adsorption of the metal monolayer results in changes in the observed rotational anisotropy patterns. For these experiments, the fundamental and second harmonic beams were both p-polarized: (a) Cu upd at a surface coverage of 0.33 monolayers; (b) Ag upd at a surface coverage of 1.0 monolayer; (c) Tl upd at a surface coverage of 0.90 monolayers. (d) Pb upd at a surface coverage of 1.0 monolayer. (Reprinted from ref 111. Copyright 1992 American Chemical Society.)

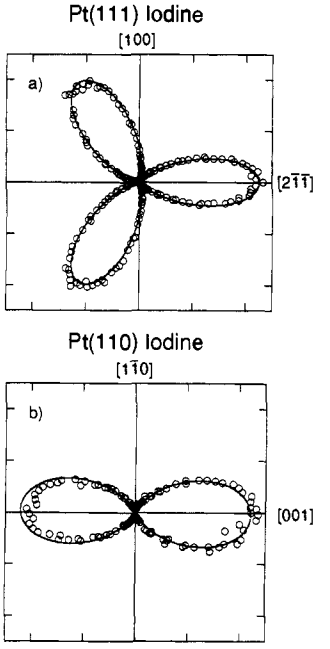

Figure 15. SHG rotational anisotropy measurements of (a) an iodine-coated Pt(111) electrode and (b) an iodine-coated Pt(110) electrode. The solid lines are fits to theoretical equations. For these experiments, the fundamental beam was s-polarized, and the second harmonic beam was p-polarized. The anisotropies are plotted in polar coordinates, with 0° corresponding to the [2$\bar{1}\bar{1}$] and [001] crystal axes for Pt(111) and Pt(110), respectively. The SHG rotational anisotropies clearly show the 3- and 2-fold symmetries of the Pt(111) and Pt(110) surfaces, respectively. (From refs 119 and 266.)

At a single-crystal metal electrode, changes in the surface electronic structure due to the presence of the upd monolayer can lead to changes in the relative magnitudes of the various elements of the surface nonlinear susceptibility ($\Delta\chi_I^{(2)}$). By measuring the SHG rotational anisotropy, a complete description of the form, magnitude, and phase of $\Delta\chi_I^{(2)}$ is obtained.[17,19]

SHG measurements have also been applied to single-crystal Pt electrodes to ascertain the average surface symmetry.[117-119,266] Figure 15, parts a and b, depict SHG rotational anisotropy measurements (plotted in polar coordinates) for Pt(111) and Pt(110) electrodes that are covered with an ordered monolayer of chemisorbed monatomic iodine.[119,266] The anisotropy plots clearly reflect the symmetry of the two surfaces, C_{3v} for the Pt(111) surface and C_{2v} for the Pt(110) surface.

While the differences in the SHG anisotropies from iodine-coated Pt(111) and Pt(110) electrodes arise from the symmetry differences of the metal substrates, different structures of a chemisorbed overlayer on the *same* single-crystal surface can also lead to changes in the overall surface symmetry. These reductions in surface symmetry upon adsorption can be monitored either with SHG rotational anisotropy experiments,[73,117,118] or with normal-incidence SHG polarization anisotropy measurements.[93,252,265]

The experimental geometry for normal-incidence polarization anisotropy measurements is depicted schematically in Figure 16a. In these experiments, the input polarization is varied from 0° to 360°, while the output polarization is fixed along one of two perpendicular crystal axes. The use of a normal-incidence geometry greatly simplifies the tensor analysis, especially for surfaces of lower symmetry. The absence of any Z component in the fundamental and second harmonic light fields restricts the surface SHG to only those surface tensor elements without a Z subscript (e.g., χ_{YYY}).

An example of a normal-incidence SHG measurement is shown in Figure 16b, which plots the SHG signal from an iodine-coated Pt(111) electrode during the potential dependent surface phase transition from a (3 × 3) to a $(\sqrt{7} \times \sqrt{7})R19.1°$ iodine monolayer.[265] The second harmonic intensity doubles as the symmetry of the electrode surface changes from C_{3v} to C_3 due to the changes in the structure of the chemisorbed monolayer. In contrast, the iodine surface coverage is found to change by less than 2% during this transition, as determined by integration of the current in the cyclic voltammogram (also shown in Figure 16b). These results clearly demonstrate the surface sensitivity of the SHG normal-incidence measurements.

The reconstruction of single-crystal metal surfaces can also be observed via the concomitant changes in surface symmetry.[108,252,262-264] For example, SHG rotational anisotropy measurements of surface reconstruction as a function of applied potential have been performed on Au(111) electrodes by Pettinger and coworkers.[113] Figure 17 plots the changes they observed in the symmetry of the SHG rotational anisotropy patterns due to a $\sqrt{3} \times 23$ reconstruction of the Au(111) electrode. In addition to changes in surface symmetry with applied potential, the adsorption of overlayers onto single-crystal electrodes can also lead to a reconstruction of the surface. The adsorbate-induced reconstruction of electrode surfaces has also been monitored with SHG rotational anisotropy measurements.[108,113]

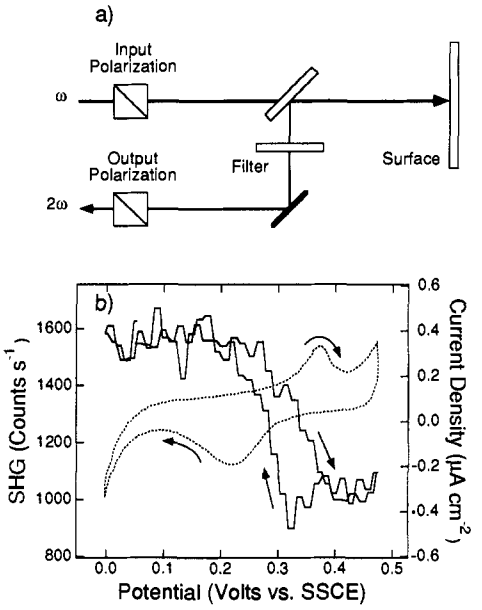

Figure 16. Normal-incidence SHG experiments of an electrochemically induced surface phase transition in iodine overlayers on a Pt(111) electrode. Part a shows the experimental geometry for normal-incidence SHG measurements. This geometry is used to significantly reduce the number of tensor elements contributing to the SHG from the surface by eliminating all those that require an electric field in the Z direction (the surface normal). Part b shows the normal-incidence SHG (—) and cyclic voltammogram (- - -) as a function of potential (vs SSCE) for a Pt(111) electrode in contact with a 0.1 mM potassium iodide solution in the region of the phase transition between the $(\sqrt{7} \times \sqrt{7})R19.1°$ and 3 × 3 iodine monolayers. The $(\sqrt{7} \times \sqrt{7})R19.1°$ monolayer exists on the surface at potentials below 0.2 V, while the 3 × 3 surface is found on the surface at potentials above 0.3 V. The use of the normal-incidence geometry results in a large change in the surface SHG signal, even though the surface coverage of chemisorbed iodine only changes by 2%. (Reprinted from ref 265. Copyright 1991 Elsevier Sequoia.)

SHG symmetry measurements at single-crystal surfaces are complicated by the fact that the SHG signal is summed in a coherent fashion over all of the domains present within the laser spot on the surface. Thus, in principle, a surface which contains equal amounts of surface domains of a lower symmetry can lead to SHG rotational anisotropy patterns that indicate a higher average surface symmetry. For example, a surface with exactly equal amounts of two domains of C_3 symmetry will lead to an SHG anisotropy pattern corresponding to an average surface symmetry of C_{3v}. More effective use of the SHG rotational anisotropy measurements in a surface symmetry determination can be made if a single-crystal surface with unequal amounts of equivalent domains is employed. The use of a stepped or vicinal single-crystal surface in SHG rotational anisotropy measurements has recently been demonstrated as a method of obtaining such a surface.[80,267-270]

D. Electric Field Measurements

In the presence of an externally applied static electric field, a bulk centrosymmetric medium can become SHG active as a result of either molecular realignment or the polarization of bonds in the sample. This process is denoted as electric field induced second harmonic generation (EFISH) and has been observed in solids,[271,272] liquids,[273,274] and gases.[273] The static electric field at an interface can also lead to an additional surface second harmonic response. In 1967, Lee et al. proposed an EFISH mechanism to explain the dependence of the surface SHG from Ag and Si electrodes on an externally applied potential.[275] The contribution of the EFISH process to the surface SHG can be written as an additional term, $\mathbf{P}_E^{(2)}(2\omega)$, in the surface nonlinear polarization:

$$\mathbf{P}_E^{(2)}(2\omega) = \chi^{(3)}:\mathbf{E}_{dc}\mathbf{E}(\omega)\mathbf{E}(\omega) \qquad (13)$$

where $\chi^{(3)}$ is the third-order nonlinear susceptibility that relates three electric fields, two at frequency ω and one at zero frequency, to the surface nonlinear polarization at frequency 2ω. In cases where the electric fields exist over an extended distance, eq 13 must be integrated over the entire interfacial region. Equation 13 predicts that in the absence of other sources, the intensity of the SHG from an interface will vary as the square of the static electric field. Thus, for cases where $\mathbf{P}_E$ dominates the surface nonlinear polarization, surface SHG measurements can be used to monitor the static electric fields at an interface. EFISH measurements of interfacial electric fields have been employed at metal,[37,84,85,87,89,90,95,96,124,126,276] semiconductor[277] and oxide surfaces.[278]

EFISH measurements of the electrostatic fields at an electrochemical interface are particularly important since chemical processes at an electrode surface are, of course, controlled primarily by the externally applied electric field. For a metal electrode in contact with a solution of high electrolyte concentration, the electric field exists only at the metal surface. From Gauss' law, the static electric field at the electrode should be directly proportional to the surface charge density σ. In 1984, Corn et al. suggested that, in the absence of specific adsorption, the potential dependent SHG from Ag electrodes could be used to monitor the surface charge density as a function of applied potential.[84,85] The potential at which $\sigma = 0$ is denoted as the potential of zero charge (pzc); determination of the pzc with SHG measurements has been performed at several electrochemical interfaces.[84,85,95,96,126,276] An example of this type of measurement by Guyot-Sionnest and Tadjeddine[126] on a Ag(111) electrode in a $KClO_4$ solution is depicted in Figure 18. The SHG shown in the figure is plotted as a function of applied potential, and exhibits a minimum at −0.7 V vs SCE. The observed minimum is identical to the pzc for the electrode as obtained from differential capacitance measurements.

EFISH measurements of electric fields have also been applied to the oxide-water interface, although the intensity of the SHG from this surface is much smaller than that observed at a metal electrode. For example, Ong et al. have measured the change in SHG from the silica-water interface as a function of bulk pH.[278] The results of this experiment are plotted in Figure 19, and show that the SHG from the interface increases dramatically with increasing bulk pH. The changes in the SHG from the interface were determined to arise from an EFISH mechanism involving the alignment of the water molecules in the diffuse double layer as a result of the charging of the silica surface by the deprotonation of -SiOH groups.

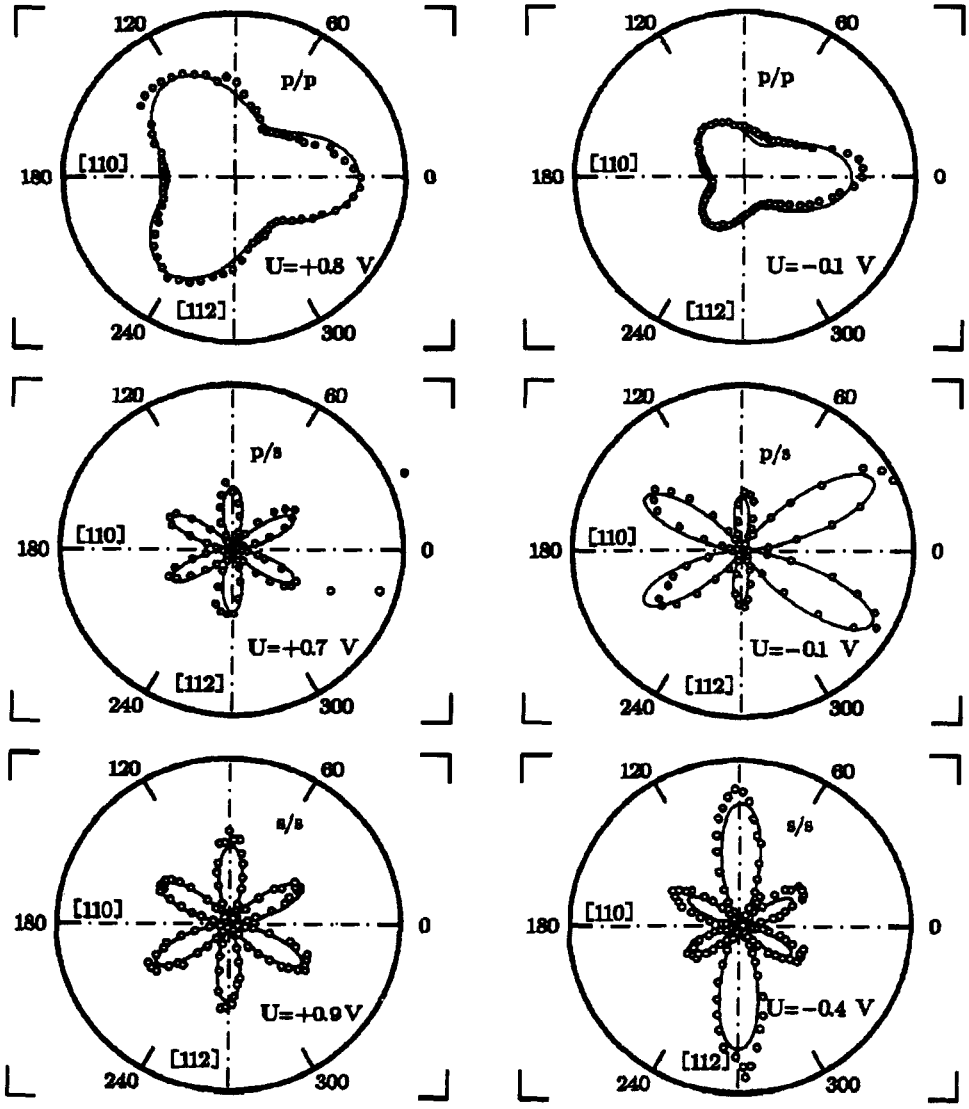

Figure 17. SHG rotational anisotropy patterns from a Au(111) electrode showing the effects of surface reconstruction on the surface symmetry. The solid lines are fits to theoretical equations. The three SHG rotational anisotropies in the left-hand column correspond to polarization combinations of p-in/p-out, p-in/s-out, and s-in/s-out for the unreconstructed Au(111) surface, which exhibits C_{3v} symmetry. The three SHG rotational anisotropies in the right-hand column were obtained at a potential where the Au(111) surface is believed to reconstruct to a $\sqrt{3} \times 23$ monolayer that has C_s symmetry. (Reprinted from ref 113. Copyright 1992 Elsevier Sequoia.)

E. Time-Resolved Studies

One of the most useful properties of the SHG from an interface is its nearly instantaneous response time. This attribute, coupled with the fact that pulsed lasers are usually employed in surface SHG experiments, has provided a relatively simple method for making time-resolved measurements of surface processes. The utility of SHG as a time-resolved method has been demonstrated at an unparalleled number of interfaces on time scales ranging from tens of seconds down to hundreds of femtoseconds. Some examples of time-resolved SHG studies include adsorption and desorption kinetics at semiconductor,[128,279,280] metal,[71,81,96,98,110,114] insulator,[177] and water[213,215] surfaces; surface diffusion measurements at liquid,[281] metal,[282,283] insulator,[164,165] and semiconductor[280,284] surfaces; surface-phase transformation measurements on Si;[252,285] photochemical reaction kinetics at liquid–air,[286] silica–air,[287–289] silica–liquid,[290] and liquid–liquid[228] interfaces; photobleaching and excited state kinetics at silica–air interfaces[287] and in Langmuir–Blodgett films;[291] underpotential deposition reaction kinetics at electrochemical interfaces;[84,98] and the reorientation of molecules at silica–air[289] and liquid–air[292,293] interfaces.

Figure 20 depicts an example of a time-resolved SHG measurement by Castro et al.[293] of the ultrafast orientational changes that occur in a monolayer of rhodamine 6G at a water–air interface during relaxation to the ground state following optical excitation. The authors have monitored the picosecond time evolution of two separate tensor elements, χ_{ZXX} and χ_{XZX}. The polarization dependence of the return of the surface SHG to its original value indicates that the orientation of rhodamine 6G in the excited sate is different from that in the ground state. Additional experiments which compared the effects of linearly polarized and circularly polarized excitation indicated that the authors were observing out-of-plane rotations in the reorientation of the dye molecules at the surface.

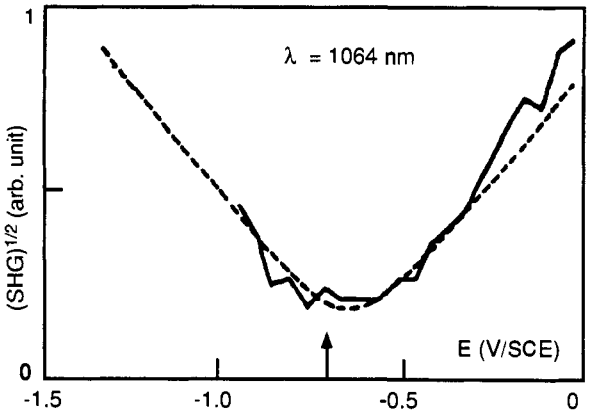

Figure 18. The square root of the SHG signal (solid line) as a function of applied potential (vs SCE) for a Ag(111) electrode in 0.1 M $KClO_4$ at a fundamental wavelength of 1064 nm. The minimum occurs very near the potential of zero charge (pzc) for this electrode (arrow). The potential dependence of the second harmonic response expected if an EFISH process at the metal–electrolyte interface is the dominant source of surface SHG is plotted in the figure as the dashed curve. (Reprinted from ref 126. Copyright 1990 American Institute of Physics.)

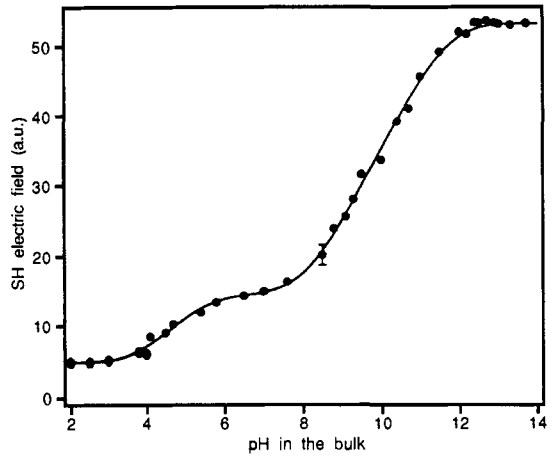

Figure 19. The square root of the surface SHG (denoted as the SH electric field) from a fused silica–water interface as a function of pH. The increase in SHG with increasing pH is attributed to an EFISH mechanism in which the static electric field in the diffuse double layer produces a preferential orientation of the water molecules at the interface. The static electric fields at the interface are controlled by the surface concentration of deprotonated surface silanol groups. The deprotonation of these surface species is a function of pH, and the curve in the figure indicates that there are two types of silanol species present on the surface. (Reprinted from ref 278. Copyright 1992 Elsevier Science Publishers.)

In addition to directly monitoring changes in the magnitude and polarization dependence of the SHG from an interface, more elaborate techniques have also been implemented in time-resolved surface SHG measurements. For example, SHG studies of surface diffusion and desorption kinetics on metal and semiconductor surfaces in UHV have employed transient gratings to create diffracted surface SHG signals. The experimental geometry used in these studies is shown schematically in Figure 21. Two beams from a high-powered pump laser are overlapped at a surface to create a spatially modulated intensity pattern which, through desorption, produces a spatially modulated adsorbate surface coverage. A second laser beam is then used to

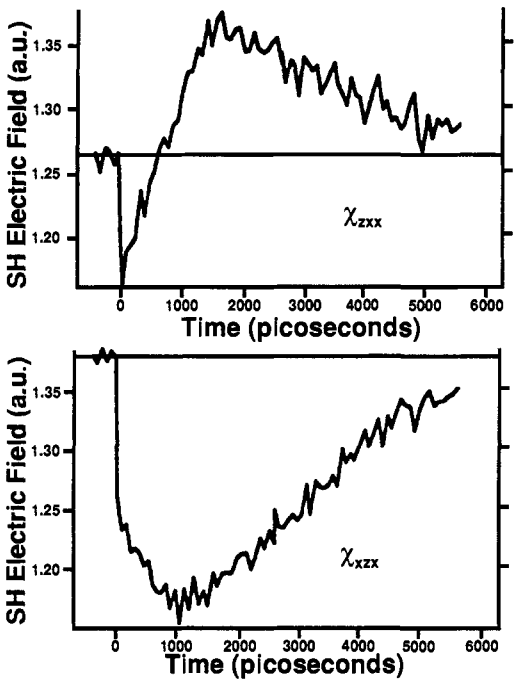

Figure 20. Time-resolved SHG measurements of χ_{ZXX} and χ_{XZX} from a monolayer of rhodamine 6G adsorbed at the water–air interface following excitation by a picosecond laser pulse. The differences observed in the evolution of χ_{ZXX} and χ_{XZX} as a function of time indicate that the rhodamine 6G molecules undergo a molecular reorientation after excitation. (Reprinted from ref 293. Copyright 1991 American Chemical Society.)

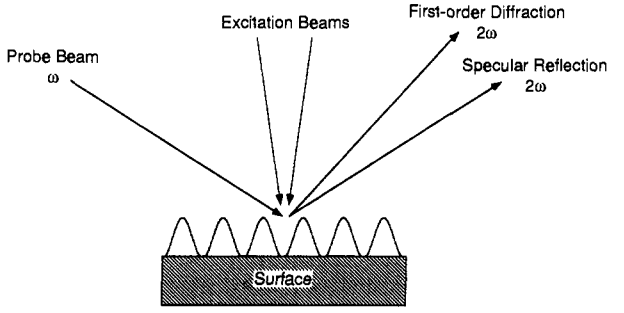

Figure 21. Schematic diagram of the experimental geometry for SHG measurements that utilize an adsorbate grating on the surface. Two beams from a high-powered pump laser are overlapped at a surface to create a spatially modulated intensity pattern which, through desorption, produces a spatially modulated adsorbate surface coverage. A second laser beam is then used to probe the surface by collecting the SHG response that is diffracted from the adsorbate grating. Because the SHG is only from the surface, the time dependence of the diffracted SHG beam intensity can be used to monitor surface diffusion kinetics.

probe the surface by collecting the SHG response that is diffracted from the adsorbate grating. Because the SHG is only from the surface, the time dependence of the diffracted SHG beam intensity can be used to monitor surface diffusion kinetics. These SHG diffraction measurements were first applied by Zhu et al. to study the diffusion of CO on Ni(111) surfaces.[282] Another example of such a measurement is shown in Figure 22, in which Reider et al. produced a monolayer grating of adsorbed hydrogen on a reconstructed Si(111) surface.[280] By assuming a linear relationship between the surface concentration of adsorbed hydrogen and the surface nonlinear susceptibility, the authors

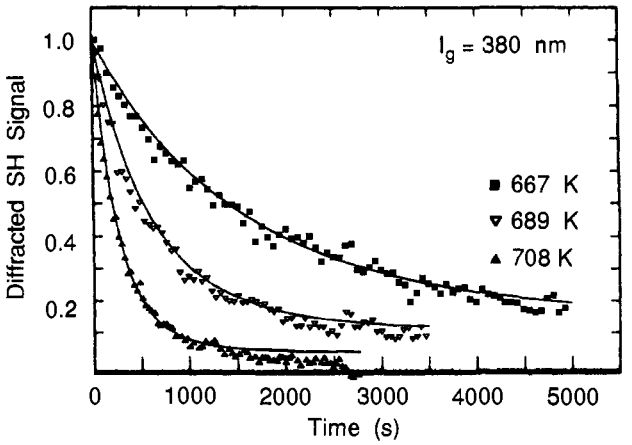

Figure 22. The time dependence of the diffracted SHG from an adsorbed hydrogen grating created on reconstructed Si-(111) surface at various surface temperatures. For this experiment, the initial surface coverage of hydrogen was 0.15 monolayers, and the period of the diffraction grating was 380 nm. The decay in the diffracted SHG results from a combination of surface diffusion and desorption. From these measurements the kinetic parameters used to describe the surface diffusion of hydrogen can be determined. (Reprinted from ref 280. Copyright 1991 American Physical Society.)

monitored the rate of surface diffusion by measuring the decay of the diffracted SHG signal. A similar work has been published for CO diffusion on Ni(110).[294]

V. Other Surface SHG Experiments and Future Directions

From the numerous examples described above, it should be evident that the surface-sensitive technique of optical second harmonic generation has proven to be extremely useful in the study of a wide variety of chemical phenomena occurring at gas–solid, gas–liquid, liquid–solid, and liquid–liquid interfaces. In this review, the various surface SHG experiments have been divided somewhat arbitrarily into studies of interfacial adsorption, molecular orientation, surface symmetry, electric field effects, and reaction/diffusion kinetics. It is difficult to incorporate everything in a review, and this list is by no means all-inclusive; for example, the many SHG experiments dealing with surface plasmons and the enhancement of electromagnetic fields at noble metal surfaces produced from gratings, roughening, or thin-film coupling have not been discussed.[89,295-314] Also not discussed is the surface-sensitive nonlinear optical technique of infrared–visible sum frequency generation, and the high-quality vibrational spectroscopic information on interfaces that has been obtained from those experiments.[315-334]

As time progresses, the application of SHG experiments to the study of interfaces will undoubtedly continue to increase and expand in several directions. Examples of some exciting new experiments include those proposed by Pan et al. and Reif et al. for the study of magnetized single-crystal surfaces,[335-337] and those by Petralli-Mallow et al.[220] in which SHG is used as a new surface-selective type of circular dichroism spectroscopy. On the theoretical side, a better quantitative understanding of the surface second harmonic response from metal surfaces will hopefully in the future improve the interpretation of the changes in the SHG signal upon chemisorption.[28,32,38,66,83] Finally, it should be noted that SHG is only the simplest of a variety of nonlinear optical experiments that can be performed at surfaces. Sum frequency generation, difference frequency generation, and five-wave mixing experiments all possess the same surface selectivity inherent in the SHG measurements, and therefore can potentially all serve as highly valuable optical probes of surface phenomena.

VI. Acknowledgments

The authors gratefully acknowledge the support of the National Science Foundation in the preparation of this review and thank the members of the Corn group for their helpful comments on the manuscript.

VII. References

(1) Shen, Y. R. *The Principles of Nonlinear Optics*; Wiley: New York, 1984.
(2) Franken, P. A.; Hill, A. E.; Peters, C. W.; Weinreich, G. *Phys. Rev. Lett.* **1961**, *7*, 118.
(3) Brown, F.; Parks, R. E.; Sleeper, A. M. *Phys. Rev. Lett.* **1965**, *14*, 1029.
(4) Bloembergen, N.; Pershan, P. S. *Phys. Rev.* **1962**, *128*, 606.
(5) Ducuing, J.; Bloembergen, N. *Phys. Rev. Lett.* **1963**, *10*, 474.
(6) Bloembergen, N.; Chang, R. K.; Jha, S. S.; Lee, C. H. *Phys. Rev.* **1968**, *174*, 813.
(7) Brown, F.; Matsuoka, M. *Phys. Rev.* **1969**, *185*, 985.
(8) Rudnick, J.; Stern, E. A. *Phys. Rev. B* **1971**, *4*, 4274.
(9) Shen, Y. R. *Annu. Rev. Mater. Sci.* **1986**, *16*, 69.
(10) Richmond, G. L.; Rojhantalab, H. M.; Robinson, J. M.; Shannon, V. L. *J. Opt. Soc. Am. B* **1987**, *4*, 228.
(11) Robinson, J. M.; Rojhantalab, H. M.; Shannon, V. L.; Koos, D. A.; Richmond, G. L. *Pure Appl. Chem.* **1987**, *59*, 1263.
(12) Richmond, G. L.; Robinson, J. M.; Shannon, V. L. *Prog. Surf. Sci.* **1988**, *28*, 1.
(13) Shen, Y. R. *Nature* **1989**, *337*, 519.
(14) Shen, Y. R. *Annu. Rev. Phys. Chem.* **1989**, *40*, 327.
(15) Heinz, T. F.; Reider, G. A. *Trac-Trends Anal. Chem.* **1989**, *8*, 235.
(16) Mcgilp, J. F. *J. Phys.: Condens. Matter* **1989**, *1*, SB85.
(17) Richmond, G. L. In *Electroanalytical Chemistry*; Bard, A. J., Ed.; Marcel Dekker, Inc.: New York, 1991; Vol. 17, pp 87.
(18) Heinz, T. F. In *Nonlinear Surface Electromagnetic Phenomena*; Ponath, H. E., Stegeman, G. I., Ed.; North-Holland: Amsterdam, 1991.
(19) Corn, R. M. *Anal. Chem.* **1991**, *63*, A285.
(20) Corn, R. M. In *Frontiers in Electrochemistry: Adsorption of Molecules at Metal Electrodes*; Lipowski, J., Ross, P. N., Ed.; VCH Publishers: New York, 1992; p 391.
(21) Eisenthal, K. B. *Annu. Rev. Phys. Chem.* **1992**, *43*, 627.
(22) Yariv, A. *Quantum Electronics*, 2nd ed.; John Wiley and Sons, Inc.: New York, 1975.
(23) Chizmeshya, A.; Zaremba, E. *Phys. Rev. B* **1988**, *37*, 2805.
(24) Schaich, W. L.; Liebsch, A. *Phys. Rev. B* **1988**, *37*, 6187.
(25) Liebsch, A. *Phys. Rev. Lett.* **1988**, *61*, 1233.
(26) Liebsch, A. *Appl. Phys. A* **1989**, *49*, 677.
(27) Liebsch, A.; Schaich, W. L. *Phys. Rev. B* **1989**, *40*, 5401.
(28) Liebsch, A. *Phys. Rev. B* **1989**, *40*, 3421.
(29) Murphy, R.; Yeganeh, M.; Song, K. J.; Plummer, E. W. *Phys. Rev. Lett.* **1989**, *63*, 318.
(30) Hu, C. D. *Phys. Rev. B* **1989**, *40*, 7520.
(31) Marlow, F. *Surf. Sci.* **1991**, *254*, L493.
(32) Dzhavakhidze, P. G.; Kornyshev, A. A.; Liebsch, A.; Urbakh, M. I. *Electrochim. Acta* **1991**, *36*, 1835.
(33) Jiang, H. B.; Li, L.; Wang, W. C.; Zheng, J. B.; Zhang, Z. M.; Chen, Z. *Phys. Rev. B* **1991**, *44*, 1220.
(34) Govorkov, S. V.; Koroteev, N. I.; Shumay, I. L.; Yakovlev, V. V. *J. Opt. Soc. Am. B* **1991**, *8*, 1023.
(35) Li, L. M.; Sun, X.; Feng, W. G. *Chin. Phys.* **1991**, *11*, 32.
(36) Petrocelli, G.; Martellucci, S.; Scudieri, F.; Agostini, A. *Appl. Phys. Lett.* **1991**, *59*, 2501.
(37) Furtak, T. E.; Tang, Y.; Simpson, L. J. *Phys. Rev. B* **1992**, *46*, 1719.
(38) Dzhavakhidze, P. G.; Kornyshev, A. A.; Liebsch, A.; Urbakh, M. *Phys. Rev. B* **1992**, *45*, 9339.
(39) Grubb, S. G.; DeSantolo, A. M.; Hall, R. B. *J. Phys. Chem.* **1988**, *92*, 1419.
(40) Hicks, J. M.; Urbach, L. E.; Plummer, E. W.; Dai, H. L. *Phys. Rev. Lett.* **1988**, *61*, 2588.
(41) Georgiadis, R.; Neff, G. A.; Richmond, G. L. *J. Chem. Phys.* **1990**, *92*, 4623.
(42) Hamilton, J. C.; Williams, L. R.; Anderson, R. J. M. *Chem. Phys. Lett.* **1990**, *167*, 507.

(43) Georgiadis, R.; Richmond, G. L. *J. Phys. Chem.* **1991**, *95*, 2895.
(44) Lindgren, S. A.; Wallden, L. *Phys. Rev. B* **1992**, *45*, 6345.
(45) Urbach, L. E.; Percival, K. L.; Hicks, J. M.; Plummer, E. W.; Dai, H. L. *Phys. Rev. B* **1992**, *45*, 3769.
(46) Heinz, T. F.; Chen, C. K.; Ricard, D.; Shen, Y. R. *Phys. Rev. Lett.* **1982**, *48*, 478.
(47) Ward, J. F. *Rev. Mod. Phys.* **1965**, *37*, 1.
(48) Li, D.; Marks, T. J.; Ratner, M. A. *Chem. Phys. Lett.* **1986**, *131*, 370.
(49) Higgins, D. A.; Abrams, M. B.; Byerly, S. B.; Corn, R. M. *Langmuir* **1992**, *8*, 1994.
(50) Chen, J. M.; Bower, J. R.; Wang, C. S.; Lee, C. H. *Opt. Commun.* **1973**, *9*, 132.
(51) Rosenzweig, Z.; Asscher, M. *Surf. Sci.* **1988**, *204*, L732.
(52) Persson, B. N. J.; Dubois, L. H. *Phys. Rev. B* **1989**, *39*, 8220.
(53) Rosenzweig, Z.; Asscher, M.; Wittenzellner, C. *Surf. Sci.* **1990**, *240*, L583.
(54) Asscher, M.; Rosenzweig, Z. *J. Vac. Sci. Tech. A* **1991**, *9*, 1913.
(55) Mizrahi, V.; Sipe, J. E. *J. Opt. Soc. Am. B* **1988**, *5*, 660.
(56) Guyot-Sionnest, P.; Chen, W.; Shen, Y. R. *Phys. Rev. B* **1986**, *33*, 8254.
(57) Tepper, P.; Zink, J. C.; Reif, J.; Matthias, E. *Phys. Rev. B* **1990**, *42*, 9685.
(58) Zhu, X. D.; Wong, A. *Phys. Rev. B* **1992**, *46*, 2540.
(59) Campbell, D. J.; Higgins, D. A.; Corn, R. M. *J. Phys. Chem.* **1990**, *94*, 3681.
(60) Higgins, D. A.; Corn, R. M. *J. Phys. Chem.* **1993**, *97*, 489.
(61) Muenchausen, R. E.; Keller, R. A.; Nogar, N. S. *J. Opt. Soc. Am. B* **1987**, *4*, 237.
(62) Tom, H. W. K.; Mate, C. M.; Zhu, X. D.; Crowell, J. E.; Heinz, T. F.; Somorjai, G. A.; Shen, Y. R. *Phys. Rev. Lett.* **1984**, *52*, 348.
(63) Tom, H. W. K.; Mate, C. M.; Zhu, X. D.; Crowell, J. E.; Shen, Y. R.; Somorjai, G. A. *Surf. Sci.* **1986**, *172*, 466.
(64) Heskett, D.; Song, K. J.; Urbach, L.; Plummer, E. W.; Burns, A.; Dai, H. L. *J. Vac. Sci. Tech. A* **1987**, *5*, 690.
(65) Heskett, D.; Urbach, L. E.; Song, K. J.; Plummer, E. W.; Dai, H. L. *Surf. Sci.* **1988**, *197*, 225.
(66) Song, K. J.; Heskett, D.; Dai, H. L.; Liebsch, A.; Plummer, E. W. *Phys. Rev. Lett.* **1988**, *61*, 1380.
(67) Li, L.; Liu, Y. H.; Yu, G. D.; Wang, W. C.; Zhang, Z. M. *Phys. Rev. B* **1989**, *40*, 10100.
(68) Liu, Y. G.; Zhang, X. X.; Chen, Z.; Wang, W. C.; Zheng, J. B.; Zhang, Z. M.; Wang, Z. J. *Chin. Phys.* **1992**, *12*, 144.
(69) Bloch, J.; Bottomley, D. J.; Janz, S.; Van Driel, H. M. *Surf. Sci.* **1991**, *257*, 328.
(70) Bradley, R. A.; Friedrich, K. A.; Wong, E. K. L.; Richmond, G. L. *J. Electroanal. Chem.* **1991**, *309*, 319.
(71) Prybyla, J. A.; Tom, H. W. K.; Aumiller, G. D. *Phys. Rev. Lett.* **1992**, *68*, 503.
(72) Heuer, W.; Schröter, L.; Zacharias, H. *Chem. Phys. Lett.* **1987**, *135*, 299.
(73) Hamilton, J. C.; Anderson, R. J. M. *Chem. Phys. Lett.* **1988**, *151*, 455.
(74) Hamilton, J. C.; Anderson, R. J. *Thin Solid Films* **1988**, *166*, 345.
(75) Anderson, R. J. M.; Hamilton, J. C. *Phys. Rev. B* **1988**, *38*, 8451.
(76) Anderson, R. J. M.; Hamilton, J. C. *High Temp. Sci.* **1989**, *26*, 1.
(77) Hamilton, J. C.; Anderson, R. J. M.; Williams, L. R. *J. Vac. Sci. Tech. B* **1989**, *7*, 1208.
(78) Zhu, X. D.; Daum, W.; Xiao, X. D.; Chin, R.; Shen, Y. R. *Phys. Rev. B* **1991**, *43*, 11571.
(79) Janz, S.; Pedersen, K.; van Driel, H. M.; Timsit, R. S. *J. Vac. Sci. Tech. A* **1991**, *9*, 1506.
(80) Janz, S.; Bottomley, D. J.; van Driel, H. M.; Timsit, R. S. *Phys. Rev. Lett.* **1991**, *66*, 1201.
(81) Rosenzweig, Z.; Asscher, M. *Surf. Sci.* **1990**, *225*, 249.
(82) Mate, C. M.; Somorjai, G. A.; Tom, H. W. K.; Zhu, X. D.; Shen, Y. R. *J. Chem. Phys.* **1988**, *88*, 441.
(83) Cini, M. *Phys. Rev. B* **1991**, *43*, 4792.
(84) Corn, R. M.; Romagnoli, M.; Levenson, M. D.; Philpott, M. R. *J. Chem. Phys.* **1984**, *81*, 4127.
(85) Corn, R. M.; Romagnoli, M.; Levenson, M. D.; Philpott, M. R. *Chem. Phys. Lett.* **1984**, *106*, 30.
(86) Richmond, G. L. *Surf. Sci.* **1984**, *147*, 115.
(87) Richmond, G. L. *Chem. Phys. Lett.* **110**, 571.
(88) Richmond, G. L. *Chem. Phys. Lett.* **1984**, *106*, 26.
(89) Richmond, G. L. *Chem. Phys. Lett.* **1985**, *113*, 359.
(90) Richmond, G. L. *Langmuir* **1986**, *2*, 132.
(91) Campbell, D. J.; Corn, R. M. *J. Phys. Chem.* **1987**, *91*, 5668.
(92) Furtak, T. E.; Korenowski, G. M.; Miragliotta, J. *Phys. Rev. B* **1987**, *35*, 2569.
(93) Miragliotta, J.; Furtak, T. E. *Phys. Rev. B* **1988**, *37*, 1028.
(94) Campbell, D. J.; Corn, R. M. *ACS Symp. Ser.* **1988**, *No. 378*, 294.
(95) Rojhantalab, H. M.; Richmond, G. L. *J. Phys. Chem.* **1989**, *93*, 3269.
(96) Robinson, J. M.; Richmond, G. L. *Electrochim. Acta.* **1989**, *34*, 1639.
(97) Miragliotta, J.; Furtak, T. E. *Surf. Interface Anal.* **1989**, *14*, 53.
(98) Robinson, J. M.; Richmond, G. L. *Chem. Phys.* **1990**, *141*, 175.
(99) Chu, P.; Richmond, G. L. *J. Electroanal. Chem.* **1990**, *296*, 203.
(100) Koos, D. A.; Shannon, V. L.; Richmond, G. L. *J. Phys. Chem.* **1990**, *94*, 2091.
(101) Shannon, V. L.; Koos, D. A.; Kellar, S. A.; Huifang, P.; Richmond, G. L. *J. Phys. Chem.* **1989**, *93*, 6434.
(102) Hewitt, T. D.; Roy, D. *Chem. Phys. Lett.* **1991**, *181*, 407.
(103) Voss, D. F.; Nagumo, M.; Goldberg, L. S.; Bunding, K. A. *J. Phys. Chem.* **1986**, *90*, 1834.
(104) Koos, D. A. *J. Electrochem. Soc.* **1989**, *136*, C218.
(105) Koos, D. A.; Richmond, G. L. *J. Chem. Phys.* **1990**, *93*, 869.
(106) Bennahmias, M. J.; Lakkaraju, S.; Stone, B. M.; Ashley, K. *J. Electroanal. Chem.* **1990**, *280*, 429.
(107) Lakkaraju, S.; Bennahmias, M. J.; Borges, G. L.; Gordon, J. G.; Lazaga, M.; Stone, B. M.; Ashley, K. *Appl. Opt.* **1990**, *29*, 4943.
(108) Friedrich, A.; Shannon, C.; Pettinger, B. *Surf. Sci.* **1991**, *251*, 587.
(109) Pettinger, B.; Friedrich, A.; Shannon, C. *Electrochim. Acta.* **1991**, *36*, 1829.
(110) Buck, M.; Eisert, F.; Fischer, J.; Grunze, M.; Trager, F. *Appl. Phys. A* **1991**, *53*, 552.
(111) Koos, D. A.; Richmond, G. L. *J. Phys. Chem.* **1992**, *96*, 3770.
(112) Pettinger, B.; Lipkowski, J.; Mirwald, S.; Friedrich, A. *Surf. Sci.* **1992**, *270*, 377.
(113) Pettinger, B.; Lipkowski, J.; Mirwald, S.; Friedrich, A. *J. Electroanal. Chem.* **1992**, *329*, 289.
(114) Buck, M.; Grunze, M.; Eisert, F.; Fischer, J.; Trager, F. *J. Vac. Sci. Tech. A* **1992**, *10*, 926.
(115) Campbell, D. J.; Corn, R. M. *J. Phys. Chem.* **1988**, *92*, 5796.
(116) Campbell, D. J.; Lynch, M. L.; Corn, R. M. *Langmuir* **1990**, *6*, 1656.
(117) Lynch, M. L.; Corn, R. M. *J. Phys. Chem.* **1990**, *94*, 4382.
(118) Lynch, M. L.; Barner, B. J.; Corn, R. M. *J. Electroanal. Chem.* **1991**, *300*, 447.
(119) Lynch, M. L.; Barner, B. J.; Lantz, J. M.; Corn, R. M. *J. Chim. Phys. Phys.-Chim. Biol.* **1991**, *88*, 1271.
(120) Biwer, B. M.; Pellin, M. J.; Schaver, M. W.; Gruen, D. M. *Surf. Sci.* **1986**, *176*, 377.
(121) Biwer, B. M.; Pellin, M. J.; Schauer, M. W.; Gruen, D. M. *Langmuir* **1988**, *4*, 121.
(122) Pellin, M. J.; Biwer, B. M.; Schauer, M. W.; Gruen, D. M. *J. Electrochem. Soc.* **1988**, *135*, C142.
(123) Biwer, B. M.; Pellin, M. J.; Schauer, M. W.; Gruen, D. M. *Surf. Interface Anal.* **1989**, *14*, 635.
(124) Werner, L.; Marlow, F.; Hill, W.; Retter, U. *Chem. Phys. Lett.* **1992**, *194*, 39.
(125) Clavilier, J. *J. Electroanal. Chem.* **1980**, *108*, 211.
(126) Guyot-Sionnest, P.; Tadjeddine, A. *J. Chem. Phys.* **1990**, *92*, 734.
(127) Chen, J. M.; Bower, J. R.; Wang, C. S. *Jpn. J. Appl. Phys. Suppl.* **1974**, *2*, 711.
(128) Reider, G. A.; Höfer, U.; Heinz, T. F. *J. Chem. Phys.* **1991**, *94*, 4080.
(129) Tom, H. W. K.; Zhu, X. D.; Shen, Y. R.; Somorjai, G. A. *Surf. Sci.* **1986**, *167*, 167.
(130) Hollering, R. W. J.; Dijkkamp, D.; Lindelauf, H. W. L.; van der Heide, P. A. M.; Krijn, M. P. C. M. *J. Vac. Sci. Tech. A* **1990**, *8*, 3997.
(131) Hollering, R. W. J.; Hoeven, A. J.; Lenssinck, J. M. *J. Vac. Sci. Tech. A* **1990**, *8*, 3194.
(132) Ghahramani, E.; Moss, D. J.; Sipe, J. E. *Phys. Rev. Lett.* **1990**, *64*, 2815.
(133) Kelly, P. V.; O'Mahony, J. D.; Rasing, T.; Mcgilp, J. F. *J. Phys.: Condens. Matter* **1991**, *3*, S193.
(134) Kelly, P. V.; O'Mahony, J. D.; Mcgilp, J. F.; Rasing, T. *Appl. Surf. Sci.* **1992**, *56–8*, 453.
(135) Kelly, P. V.; O'Mahony, J. D.; Mcgilp, J. F.; Rasing, T. *Surf. Sci.* **1992**, *270*, 849.
(136) Patterson, C. H.; Weaire, D.; Mcgilp, J. F. *J. Phys.: Condens. Matter* **1992**, *4*, 4017.
(137) Kelly, P. V.; Tang, Z. R.; Woolf, D. A.; Williams, R. H.; Mcgilp, J. F. *Surf. Sci.* **1991**, *251*, 87.
(138) Mcgilp, J. F.; Yeh, Y. *Solid State Commun.* **1986**, *59*, 91.
(139) Mcgilp, J. F. *J. Vac. Sci. Tech. A* **1987**, *5*, 1442.
(140) O'Mahony, J. D.; Kelly, P. V.; Mcgilp, J. F. *Appl. Surf. Sci.* **1992**, *56–8*, 449.
(141) Kulyuk, L. L.; Shutov, D. A.; Strumban, E. E.; Aktsipetrov, O. A. *J. Opt. Soc. Am. B* **1991**, *8*, 1766.
(142) Hollering, R. W. J.; Dijkkamp, D.; Lindelauf, H. W. L.; van der Heide, P. A. M. *J. Vac. Sci. Tech B* **1991**, *9*, 1967.
(143) Heinz, T. F.; Himpsel, F. J.; Palange, E.; Burstein, E. *Phys. Rev. Lett.* **1989**, *63*, 644.
(144) Schultz, K. A.; Suni, I. I.; Allen, C. E.; Seebauer, E. G. *Surf. Sci.* **1992**, *276*, 40.
(145) Stehlin, T.; Feller, M.; Guyot-Sionnest, P.; Shen, Y. R. *Opt. Lett.* **1988**, *13*, 389.
(146) Buhaenko, D. S.; Francis, S. M.; Goulding, P. A.; Pemble, M. E. *J. Crystal Growth* **1989**, *97*, 595.
(147) Buhaenko, D. S.; Francis, S. M.; Goulding, P. A.; Pemble, M. E. *J. Phys.: Condens. Matter* **1989**, *1*, B251.
(148) Armstrong, S. R.; Pemble, M. E.; Stafford, A.; Taylor, A. G. *J. Phys.: Condens. Matter* **1991**, *3*, S363.
(149) Pemble, M. E.; Stafford, A.; Taylor, A. G. *Appl. Surf. Sci.* **1992**, *54*, 490.
(150) Armstrong, S. R.; Hoare, R. D.; Pemble, M. E.; Povey, I. M.; Stafford, A.; Taylor, A. G. *J. Crystal Growth* **1992**, *120*, 94.

(151) Hollering, R. W. J. *Opt. Commun.* **1992**, *90*, 147.
(152) Heinz, T. F.; Tom, H. W. K.; Shen, Y. R. *Phys. Rev. A* **1983**, *28*, 1883.
(153) Marowsky, G.; Gierulski, A.; Dick, B. *Opt. Commun.* **1985**, *52*, 339.
(154) Cresswell, S. A.; Steehler, J. K. *Appl. Spectrosc.* **1987**, *41*, 1329.
(155) Marowsky, G.; Chi, L. F.; Möbius, D.; Steinhoff, R.; Shen, Y. R.; Dorsch, D.; Rieger, B. *Chem. Phys. Lett.* **1988**, *147*, 420.
(156) Steinhoff, R.; Chi, L. F.; Marowsky, G.; Möbius, D. *J. Opt. Soc. Am. B* **1989**, *6*, 843.
(157) Berkovic, G.; Shen, Y. R.; Marowsky, G.; Steinhoff, R. *J. Opt. Soc. Am. B* **1989**, *6*, 205.
(158) Hollering, R. W. J.; Vrehen, Q. H. F.; Marowsky, G. *Opt. Commun.* **1990**, *78*, 387.
(159) Werner, L.; Hill, W.; Marlow, F.; Glismann, A.; Hertz, O. *Thin Solid Films* **1991**, *205*, 58.
(160) Higgins, D. A.; Byerly, S. K.; Abrams, M. B.; Corn, R. M. *J. Phys. Chem.* **1991**, *95*, 6984.
(161) Carpenter, M. A.; Willand, C. S.; Penner, T. L.; Williams, D. J.; Mukamel, S. *J. Phys. Chem.* **1992**, *96*, 2801.
(162) Hill, W.; Werner, L.; Marlow, F. *Ber. Bunsen.-Ges. Phys. Chem.* **1991**, *95*, 1453.
(163) Marlow, F.; Werner, L.; Hill, W. *Surf. Sci.* **1991**, *249*, 365.
(164) Zhang, J. Y.; Shen, Y. R.; Soane, D. S.; Freilich, S. C. *Appl. Phys. Lett.* **1991**, *59*, 1305.
(165) Zhang, J. Y.; Shen, Y. R.; Soane, D. S. *J. Appl. Phys.* **1992**, *71*, 2655.
(166) Pinnow, M.; Marowsky, G.; Sieverdes, F.; Möbius, D.; Krohnke, C.; Neuschafer, D. *Thin Solid Films* **1992**, *210*, 231.
(167) Gao, J. P.; Darling, G. D. *J. Am. Chem. Soc.* **1992**, *114*, 3997.
(168) Ye, P.; Shen, Y. R. *Phys. Rev. B* **1983**, *28*, 4288.
(169) Hayden, L. M. *Phys. Rev. B* **1988**, *38*, 3718.
(170) Xiao, X. D.; Vogel, V.; Shen, Y. R.; Marowsky, G. *J. Chem. Phys.* **1991**, *94*, 2315.
(171) Guyot-Sionnest, P.; Shen, Y. R. *Phys. Rev. B* **1988**, *38*, 7985.
(172) Reider, G. A.; Huemer, M.; Schmidt, A. J. *Opt. Commun.* **1988**, *68*, 149.
(173) Heinz, T. F.; DiVincenzo, D. P. *Phys. Rev. A* **1990**, *42*, 6249.
(174) Rief, J.; Tepper, P.; Zink, J. C.; Wassermann, B.; Mirbt, S.; Matthias, E. *Vacuum* **1990**, *41*, 1646.
(175) Tepper, P.; Zink, J. C.; Schmelz, H.; Wassermann, B.; Reif, J.; Matthias, E. *J. Vac. Sci. Tech. B* **1989**, *7*, 1212.
(176) Berkovic, G. *Physica A* **1990**, *168*, 140.
(177) Yerushalmi-Rozen, R.; Klein, J.; Berkovic, G. *Langmuir* **1992**, *8*, 1392.
(178) Nonlinear *Optical Properties of Organic Molecules and Crystals*; Chemla, D. S., Zyss, J., Ed.; Academic Press: Orlando, 1987.
(179) Prasad, P. N.; Williams, D. J. *Introduction to Nonlinear Optical Effects in Molecules and Polymers*; Wiley: New York, 1991.
(180) Aktsipetrov, O. A.; Akhmediev, N. N.; Baranova, I. M.; Mishina, E. D.; Novak, V. R. *Sov. Phys. JETP* **1985**, *62*, 524.
(181) Marowsky, G.; Steinhoff, R. *Opt. Lett.* **1988**, *13*, 707.
(182) Marowsky, G.; Steinhoff, R.; Chi, L. F.; Hutter, J.; Wagniere, G. *Phys. Rev. B* **1988**, *38*, 6274.
(183) Hayden, L. M.; Anderson, B. L.; Lam, J. Y. S.; Higgins, B. G.; Stroeve, P.; Kowel, S. T. *Thin Solid Films* **1988**, *160*, 379.
(184) Schildkraut, J. S.; Penner, T. L.; Willand, C. S.; Ulman, A. *Opt. Lett.* **1988**, *13*, 134.
(185) Mizrahi, V.; Stegeman, G. I.; Knoll, W. *Chem. Phys. Lett.* **1989**, *156*, 392.
(186) Shen, Y. R. *Liq. Cryst.* **1989**, *5*, 635.
(187) Chen, W.; Feller, M. B.; Shen, Y. R. *Phys. Rev. Lett.* **1989**, *63*, 2665.
(188) Nakamura, K.; Era, M.; Tsutsui, T.; Saito, S. *Jpn. J. Appl. Phys.* **1990**, *29*, L628.
(189) Kajikawa, K.; Shirota, K.; Takezoe, H.; Fukuda, A. *Jpn. J. Appl. Phys.* **1990**, *29*, 913.
(190) Kajikawa, K.; Kigata, K.; Takezoe, H.; Fukuda, A. *Mol. Cryst. Liq. Cryst.* **1990**, *182*, 91.
(191) Kurata, T.; Tsumura, A.; Fuchigami, H.; Koezuka, H. *J. Phys. Chem.* **1991**, *95*, 8831.
(192) Nalwa, H. S.; Nakajima, K.; Watanabe, T.; Nakamura, K.; Yamada, A.; Miyata, S. *Jpn. J. Appl. Phys.* **1991**, *30*, 983.
(193) Kajikawa, K.; Takezoe, H.; Fukuda, A. *Jpn. J. Appl. Phys.* **1991**, *30*, 1050.
(194) Barmentlo, M.; Hoekstra, F. R.; Willard, N. P.; Hollering, R. W. J. *Phys. Rev. A* **1991**, *43*, 5740.
(195) Verbiest, T.; Samyn, C.; Persoons, A. *Thin Solid Films* **1992**, *210*, 188.
(196) Kajikawa, K.; Anzai, T.; Takezoe, H.; Fukuda, A.; Okada, S.; Matsuda, H.; Nakanishi, H.; Abe, T.; Ito, H. *Chem. Phys. Lett.* **1992**, *192*, 113.
(197) Kajikawa, K.; Anzai, T.; Shirota, K.; Takezoe, H.; Fukuda, A. *Thin Solid Films* **1992**, *210*, 699.
(198) Kajikawa, K.; Yamaguchi, T.; Anzai, T.; Takezoe, H.; Fukuda, A.; Okada, S.; Matsuda, H.; Nakanishi, H.; Abe, T.; Ito, H. *Langmuir* **1992**, *8*, 2764.
(199) Miyamoto, Y.; Kaifu, K.; Koyano, T.; Saito, M.; Kato, M. *Langmuir* **1992**, *8*, 769.
(200) Miyamoto, Y.; Kaifu, K.; Koyano, T.; Saito, M.; Kato, M. *Thin Solid Films* **1992**, *210*, 178.
(201) Ashwell, G. J.; Hargreaves, R. C.; Baldwin, C. E.; Bahra, G. S.; Brown, C. R. *Nature* **1992**, *357*, 393.
(202) Dentan, V.; Blanchard-Desce, M.; Palacin, S.; Ledoux, I.; Barraud, A.; Lehn, J. M.; Zyss, J. *Thin Solid Films* **1992**, *210*, 221.
(203) Geisler, T.; Rosenkilde, S.; Ramanujam, P. S.; Wijekoon, W. M. K. P.; Prasad, P. N. *Phys. Scr.* **1992**, *46*, 127.
(204) Barmentlo, M.; van Aerle, N. A. J. M.; Hollering, R. W. J.; Damen, J. P. M. *J. Appl. Phys.* **1992**, *71*, 4799.
(205) Su, W. F. A.; Kurata, T.; Nobutoki, H.; Koezuka, H. *Langmuir* **1992**, *8*, 915.
(206) Koga, T.; Kawazumi, H.; Nagamura, T.; Ogawa, T. *Anal. Sci.* **1992**, *8*, 259.
(207) Wang, C. C. *Phys. Rev.* **1969**, *178*, 1457.
(208) Rasing, T.; Shen, Y. R.; Kim, M. W.; Grubb, S. *Phys. Rev. Lett.* **1985**, *55*, 2903.
(209) Rasing, T.; Shen, Y. R.; Kim, M. W.; Valint, P., Jr.; Bock, J. *Phys. Rev. A* **1985**, *31*, 537.
(210) Castro, A.; Bhattacharyya, K.; Eisenthal, K. B. *J. Chem. Phys.* **1991**, *95*, 1310.
(211) Rasing, T.; Berkovic, G.; Shen, Y. R.; Grubb, S. G.; Kim, M. W. *Chem. Phys. Lett.* **1986**, *130*, 1.
(212) Hicks, J. M.; Kemnitz, K.; Eisenthal, K. B.; Heinz, T. F. *J. Phys. Chem.* **1986**, *90*, 560.
(213) Rasing, T.; Stehlin, T.; Shen, Y. R.; Kim, M. W.; Valint, P., Jr. *J. Chem. Phys.* **1988**, *89*, 3386.
(214) Bhattacharyya, K.; Castro, A.; Sitzmann, E. V.; Eisenthal, K. B. *J. Chem. Phys.* **1988**, *89*, 3376.
(215) Castro, A.; Ong, S. W.; Eisenthal, K. B. *Chem. Phys. Lett.* **1989**, *163*, 412.
(216) Zhao, X.; Goh, M. C.; Eisenthal, K. B. *J. Phys. Chem.* **1990**, *94*, 2222.
(217) Weissbuch, I.; Berkovic, G.; Leiserowitz, L.; Lahav, M. *J. Am. Chem. Soc.* **1990**, *112*, 5874.
(218) Vogel, V.; Mullin, C. S.; Shen, Y. R.; Kim, M. W. *J. Chem. Phys.* **1991**, *95*, 4620.
(219) Vogel, V.; Mullin, C. S.; Shen, Y. R. *Langmuir* **1991**, *7*, 1222.
(220) Petralli-Mallow, T.; Wong, T. M.; Byers, J. D.; Yee, H. I.; Hicks, J. M. *J. Phys. Chem.* **1993**, *97*, 1383.
(221) Weissbuch, I.; Popovitz-Biro, R.; Wang, J.; Berkovic, G.; Leiserowitz, L.; Lahav, M. *Pure Appl. Chem.* **1992**, *64*, 1263.
(222) Bhattacharyya, K.; Sitzmann, E. V.; Eisenthal, K. B. *J. Chem. Phys.* **1987**, *87*, 1442.
(223) Xiao, X. D.; Vogel, V.; Shen, Y. R. *Chem. Phys. Lett.* **1989**, *163*, 555.
(224) Zhao, X.; Subrahmanyan, S.; Eisenthal, K. B. *Chem. Phys. Lett.* **1990**, *171*, 558.
(225) Grubb, S. G.; Kim, M. W.; Rasing, T.; Shen, Y. R. *Langmuir* **1988**, *4*, 452.
(226) Bell, A. J.; Frey, J. G.; Vandernoot, T. J. *J. Chem. Soc., Faraday Trans.* **1992**, *88*, 2027.
(227) Bavli, R.; Yogev, D.; Efrima, S.; Berkovic, G. *J. Phys. Chem.* **1991**, *95*, 7422.
(228) Kott, K. L.; Higgins, D. A.; McMahon, R. J.; Corn, R. M. *J. Am. Chem. Soc.* **1993**, *115*, 5342.
(229) Zhang, T. G.; Zhang, C. H.; Wong, G. K. *J. Opt. Soc. Am. B* **1990**, *7*, 902.
(230) Guyot-Sionnest, P.; Shen, Y. R.; Heinz, T. F. *Appl. Phys. B* **1987**, *42*, 237.
(231) Oudar, J. A.; Zyss, J. *Phys. Rev. A* **1982**, *26*, 2016.
(232) Mazely, T. L.; Hetherington, W. M. *J. Chem. Phys.* **1987**, *86*, 3640.
(233) Pariser, R.; Parr, R. G. *J. Chem. Phys.* **1953**, *21*, 466.
(234) Pople, J. A. *Trans. Faraday Soc.* **1953**, *49*, 1375.
(235) Pariser, R.; Parr, R. G. *J. Chem. Phys.* **1953**, *21*, 767.
(236) Pariser, R. *J. Chem. Phys.* **1953**, *21*, 568.
(237) Li, D.; Ratner, M. A.; Marks, T. J. *J. Am. Chem. Soc.* **1988**, *110*, 1707.
(238) Hollering, R. W. J.; Teesselink, W. J. O. V. *Opt. Commun.* **1990**, *79*, 224.
(239) *Molecular Orientation in Thin Films as Probed by Optical Second Harmonic Generation*; Corn, R. M., Higgins, D. A., Ed.; Manning Publishers: Greenwich, CT, submitted for publication; Vol. 6.
(240) Di Lazzaro, P.; Mataloni, P.; DeMartini, F. *Chem. Phys. Lett.* **1985**, *114*, 103.
(241) Peterson, E. S.; Harris, C. B. *J. Chem. Phys.* **1989**, *91*, 2683.
(242) Goh, M. C.; Eisenthal, K. B. *Chem. Phys. Lett.* **1989**, *157*, 101.
(243) Hsiung, H.; Meredith, G. R.; Vanherzeele, H.; Popovitz-Biro, R.; Shavit, E.; Lahav, M. *Chem. Phys. Lett.* **1989**, *164*, 539.
(244) Shirota, K.; Kajikawa, K.; Takezoe, H.; Fukuda, A. *Jpn. J. Appl. Phys.* **1990**, *29*, 750.
(245) Kemnitz, K.; Bhattacharyya, K.; Hicks, J. M.; Pinto, G. R.; Eisenthal, K. B.; Heinz, T. F. *Chem. Phys. Lett.* **1986**, *131*, 285.
(246) Goh, M. C.; Hicks, J. M.; Kemnitz, K.; Pinto, G. R.; Bhattacharyya, K.; Eisenthal, K. B.; Heinz, T. F. *J. Phys. Chem.* **1988**, *92*, 5074.
(247) Sato, O.; Baba, R.; Hashimoto, K.; Fujishima, A. *J. Phys. Chem.* **1991**, *95*, 9636.
(248) Sato, O.; Baba, R.; Hashimoto, K.; Fujishima, A. *J. Electroanal. Chem.* **1991**, *306*, 291.
(249) Guidotti, D.; Driscoll, T. A.; Gerritsen, H. J. *Solid State Commun.* **1983**, *46*, 337.
(250) Driscoll, T. A.; Guidotti, D. *Phys. Rev. B* **1983**, *28*, 1171.

(251) Tom, H. W. K.; Heinz, T. F.; Shen, Y. R. *Phys. Rev. Lett.* **1983**, *51*, 1983.
(252) Heinz, T. F.; Loy, M. M. T.; Thompson, W. A. *Phys. Rev. Lett.* **1985**, *54*, 63.
(253) Heinz, T. F.; Loy, M. M. T.; Thompson, W. A. *J. Vac. Sci. Tech. B* **1985**, *3*, 1467.
(254) Tom, H. W. K.; Aumiller, G. D. *Phys. Rev. B* **1986**, *33*, 8818.
(255) Hollering, R. W. J. *J. Opt. Soc. Am. B* **1991**, *8*, 374.
(256) Bradley, R. A.; Arekat, S.; Georgiadis, R.; Robinson, J. M.; Kevan, S. D.; Richmond, G. L. *Chem. Phys. Lett.* **1990**, *168*, 468.
(257) Hoffbauer, M. A.; McVeigh, V. J.; Zuerlein, M. J. *J. Vac. Sci. Tech. B* **1992**, *10*, 268.
(258) Shannon, V. L.; Koos, D. A.; Richmond, G. L. *J. Phys. Chem.* **1987**, *91*, 5548.
(259) Shannon, V. L.; Koos, D. A.; Richmond, G. L. *Appl. Opt.* **1987**, *26*, 3579.
(260) Shannon, V. L.; Koos, D. A.; Richmond, G. L *J. Chem. Phys.* **1987**, *87*, 1440.
(261) Shannon, V. L.; Koos, D. A.; Robinson, J. M.; Richmond, G. L. *Chem. Phys. Lett.* **1987**, *142*, 323.
(262) Friedrich, A.; Pettinger, B.; Kolb, D. M.; Lüpke, G.; Steinhoff, R.; Marowsky, G. *Chem. Phys. Lett.* **1989**, *163*, 123.
(263) Lüpke, G.; Marowsky, G.; Steinhoff, R.; Friedrich, A.; Pettinger, B.; Kolb, D. M. *Phys. Rev. B* **1990**, *41*, 6913.
(264) Tang, Y.; Simpson, L. J.; Furtak, T. E. *Phys. Rev. Lett.* **1991**, *67*, 2814.
(265) Lynch, M. L.; Corn, R. M. *J. Electroanal. Chem.* **1991**, *318*, 379.
(266) Lantz, J. M.; Corn, R. M. Unpublished Results.
(267) Van Hasselt, C. W.; Verheijen, M. A.; Rasing, T. *Phys. Rev. B* **1990**, *42*, 9263.
(268) Verheijen, M. A.; van Hasselt, C. W.; Rasing, T. *Surf. Sci.* **1991**, *251*, 467.
(269) Hollering, R. W. J.; Dijkkamp, D.; Elswijk, H. B. *Surf. Sci.* **1991**, *243*, 121.
(270) Hollering, R. W. J.; Barmentlo, M. *Opt. Commun.* **1992**, *88*, 141.
(271) Terhune, R. W.; Maker, P. D.; Savage, C. M. *Phys. Rev. Lett.* **1962**, *8*, 404.
(272) Minck, R. W.; Terhune, R. W.; Wang, C. C. *Appl. Opt.* **1966**, *5*, 1595.
(273) Mayer, G. *Acad. Sci. B* **1968**, 267, 54.
(274) Levine, B. F.; Bethea, C. G. *J. Chem. Phys.* **1975**, *63*, 2666.
(275) Lee, C. H.; Chang, R. K.; Bloembergen, N. *Phys. Rev. Lett.* **1967**, *18*, 167.
(276) Tadjeddine, A.; Guyot-Sionnest, P. *J. Phys. Chem.* **1990**, *94*, 5193.
(277) Lantz, J. M.; Baba, R.; Corn, R. M. *J. Phys. Chem.* **1993**, *97*, 7392.
(278) Ong, S.; Zhao, X.; Eisenthal, K. B. *Chem. Phys. Lett.* **1992**, *191*, 327.
(279) Pemble, M. E.; Allen, J. T.; Buhaenko, D. S.; Francis, S. M.; Goulding, P. A.; Lee, J.; Parrott, M. J. *Appl. Surf. Sci.* **1990**, *46*, 32.
(280) Reider, G. A.; Höfer, U.; Heinz, T. F. *Phys. Rev. Lett.* **1991**, *66*, 1994.
(281) Zhao, X.; Goh, M. C.; Subrahmanyan, S.; Eisenthal, K. B. *J. Phys. Chem.* **1990**, *94*, 3370.
(282) Zhu, X. D.; Rasing, T.; Shen, Y. R. *Phys. Rev. Lett.* **1988**, *61*, 2883.
(283) Zhu, X. D.; Shen, Y. R. *Opt. Lett.* **1989**, *14*, 503.
(284) Suzuki, T.; Heinz, T. F. *Opt. Lett.* **1989**, *14*, 1201.
(285) Tom, H. W. K.; Aumiller, G. D.; Brito-Cruz, C. H. *Phys. Rev. Lett.* **1988**, *60*, 1438.
(286) Sitzmann, E. V.; Eisenthal, K. B. *J. Phys. Chem.* **1988**, *92*, 4579.
(287) Meech, S. R.; Yoshihara, K. *Chem. Phys. Lett.* **1989**, *154*, 20.
(288) Meech, S. R.; Yoshihara, K. *J. Phys. Chem.* **1990**, *94*, 4913.
(289) Meech, S. R.; Yoshihara, K. *Photochem. Photobiol.* **1991**, *53*, 627.
(290) Meech, S. R.; Yoshihara, K. *Chem. Phys. Lett.* **1990**, *174*, 423.
(291) Hsiung, H. *Appl. Phys. Lett.* **1991**, *59*, 2495.
(292) Zhao, X. L.; Subrahmanyan, S.; Eisenthal, K. B. *Phys. Rev. Lett.* **1991**, *67*, 2025.
(293) Castro, A.; Sitzmann, E. V.; Zhang, D.; Eisenthal, K. B. *J. Phys. Chem.* **1991**, *95*, 6752.
(294) Xiao, X.-D.; Zhu, X. D.; Daum, W.; Shen, Y. R. *Phys. Rev. Lett.* **1991**, *66*, 2352.
(295) Chen, C. K.; Heinz, T. F.; Ricard, D.; Shen, Y. R. *Phys. Rev. B* **1983**, *27*, 1965.
(296) Boyd, G. T.; Rasing, T.; Leite, J. R. R.; Shen, Y. R. *Phys. Rev. B* **1984**, *30*, 519.
(297) Aktsipetrov, O. A.; Dubinina, E. M.; Elovikov, S. S.; Mishna, E. D.; Nikulin, A. A.; Novikova, N. N.; Strebkov, M. S. *JETP Lett.* **1988**, *48*, 97.
(298) Cui, D. F.; Chen, Z. H.; Gu, S. J.; Lu, H. B.; Zhou, Y. L.; Yang, G. Z. *Phys. Scr.* **1988**, *37*, 746.
(299) Quail, J. C.; Simon, H. J. *J. Opt. Soc. Am. B* **1988**, *5*, 325.
(300) Reinisch, R.; Neviere, M.; Akhouayri, H.; Coutaz, J. L.; Maystre, D.; Pic, E. *Opt. Eng.* **1988**, *27*, 961.
(301) Simon, H. J.; Huang, C.; Quail, J. C.; Chen, Z. *Phys. Rev. B* **1988**, *38*, 7408.
(302) Zhan, C.; Simon, H. J. *Opt. Lett.* **1988**, *13*, 1008.
(303) Simon, H. J.; Chen, Z. *Phys. Rev. B* **1989**, *39*, 3077.
(304) Aktsipetrov, O. A.; Dubinina, E. M.; Elovikov, S. S.; Mishna, E. D.; Nikulin, A. A.; Novikova, N. N.; Strebkov, M. S. *Solid State Commun.* **1989**, *70*, 1021.
(305) Haller, K. L.; Bumm, L. A.; Altkorn, R. I.; Zeman, E. J.; Schatz, G. C.; Van Duyne, R. P. *J. Chem. Phys.* **1989**, *90*, 1237.
(306) Li, L.; Liu, Y. H.; Yu, G. D.; Wang, W. C.; Zhang, Z. M. *Phys. Rev. B* **1989**, *39*, 8728.
(307) Schmidlin, E. M.; Simon, H. J. *Appl. Opt.* **1989**, *28*, 3323.
(308) Tzeng, C. C.; Lue, J. T. *Surf. Sci.* **1989**, *216*, 579.
(309) Aktsipetrov, O. A.; Nikulin, A. A.; Panov, V. I.; Vasilev, S. I. *Solid State Commun.* **1990**, *73*, 411.
(310) Aktsipetrov, O. A.; Nikulin, A. A.; Panov, V. I.; Vasilev, S. I.; Petukhov, A. V. *Solid State Commun.* **1990**, *76*, 55.
(311) Leitner, A. *Mol. Phys.* **1990**, *70*, 197.
(312) Li, G. F.; Seshadri, S. R. *Phys. Rev. B* **1991**, *44*, 1240.
(313) Wang, X. J.; Simon, H. J. *Opt. Lett.* **1991**, *16*, 1475.
(314) Simon, H. J.; Wang, Y.; Zhou, L. B.; Chen, Z. *Opt. Lett.* **1992**, *17*, 1268.
(315) Zhu, X. D.; Suhr, H.; Shen, Y. R. *Phys. Rev. B* **1987**, *35*, 3047.
(316) Hunt, J. H.; Guyot-Sionnest, P.; Shen, Y. R. *Chem. Phys. Lett.* **1987**, *133*, 189.
(317) Harris, A. L.; Chidsey, C. E. D.; Levinos, N. J.; Loiacono, D. N. *Chem. Phys. Lett.* **1987**, *141*, 350.
(318) Guyot-Sionnest, P.; Hunt, J. H.; Shen, Y. R. *Phys. Rev. Lett.* **1987**, *59*, 1597.
(319) Superfine, R.; Guyot-Sionnest, P.; Hunt, J. H.; Kao, C. T.; Shen, Y. R. *Surf. Sci.* **1988**, *200*, L445.
(320) Guyot-Sionnest, P.; Superfine, R.; Hunt, J. H.; Shen, Y. R. *Chem. Phys. Lett.* **1988**, *144*, 1.
(321) Harris, A. L.; Levinos, N. J. *J. Chem. Phys.* **1989**, *90*, 3878.
(322) Superfine, R.; Huang, J. Y.; Shen, Y. R. *Opt. Lett.* **1990**, *15*, 1276.
(323) Superfine, R.; Huang, J. Y.; Shen, Y. R. *Chem. Phys. Lett.* **1990**, *172*, 303.
(324) Guyot-Sionnest, P.; Dumas, P.; Chabal, Y. J. *J. Electron Spectrosc. Rel. Phenom.* **1990**, *54*, 27.
(325) Guyot-Sionnest, P.; Tadjeddine, A. *Chem. Phys. Lett.* **1990**, *172*, 341.
(326) Guyot-Sionnest, P. *Ann. Phys.* **1990**, *15*, 89.
(327) Miragliotta, J.; Polizotti, R. S.; Rabinowitz, P.; Cameron, S. D.; Hall, R. B. *Appl. Phys. A* **1990**, *51*, 221.
(328) Miragliotta, J.; Polizzotti, R. S.; Rabinowitz, P.; Cameron, S. D.; Hall, R. B. *Chem. Phys.* **1990**, *143*, 123.
(329) Harris, A. L.; Rothberg, L.; Dubois, L. H.; Levinos, N. J.; Dhar, L. *Phys. Rev. Lett.* **1990**, *64*, 2086.
(330) Tadjeddine, A.; Guyot-Sionnest, P. *Electrochim. Acta* **1991**, *36*, 1849.
(331) Bain, C. D.; Davies, P. B.; Ong, T. H.; Ward, R. N.; Brown, M. A. *Langmuir* **1991**, *7*, 1563.
(332) Harris, A. L.; Rothberg, L. *J. Chem. Phys.* **1991**, *94*, 2449.
(333) Morin, M.; Levinos, N. J.; Harris, A. L. *J. Chem. Phys.* **1992**, *96*, 3950.
(334) Morin, M.; Jakob, P.; Levinos, N. J.; Chabal, Y. J.; Harris, A. L. *J. Chem. Phys.* **1992**, *96*, 6203.
(335) Pan, R.-P.; Shen, Y. R. *Chin. J. Phys.* **1987**, *25*, 175.
(336) Pan, R. P.; Wei, H. D.; Shen, Y. R. *Phys. Rev. B* **1989**, *39*, 1229.
(337) Reif, J.; Zink, J. C.; Schneider, C. M.; Kirschner, J. *Phys. Rev. Lett.* **1991**, *67*, 2878.